DALTON

Halide-bridged arsine- and phosphine-capped diruthenium complexes, $[(R_3As)_3Ru(\mu\text{-}X)_3Ru(AsR_3)_3]^+$ and $[(R_3P)_3Ru(\mu\text{-}X)_3Ru(PR_3)_3]^+$ (X = Cl or Br), as precursors to confacial mixed-valence ruthenium 'blues': spectroelectrochemical studies spanning the binuclear oxidation states II,II, II,III and III,III

Brett D. Yeomans, David G. Humphrey and Graham A. Heath*

The Research School of Chemistry, The Australian National University, Canberra ACT 0200, Australia

A series of six tertiary-arsine-capped binuclear complexes, $[L_3Ru(\mu\text{-}X)_3RuL_3][CF_3SO_3]$ (L = $AsMe_3$, $AsMe_2Ph$ or $AsMePh_2$; X = Cl or Br) together with a full range of purely PR_3-capped analogues and the mixed-ligand complex $[(Ph_3P)(Me_3As)_2Ru(\mu\text{-}Cl)_3Ru(AsMe_3)_2(PPh_3)][CF_3SO_3]$ have been characterised. The previously neglected arsine-capped compounds share the well defined electrochemical behaviour of their phosphine congeners. Stepwise reversible oxidations connect the $Ru_2^{II,II}$ closed-shell d^6d^6 (=12-e) resting state with the d^5d^6 (11-e) and d^5d^5 (10-e) levels, and all the mixed-valence $[L_3Ru(\mu\text{-}X)_3RuL_3]^{2+}$ species can be characterised through electrogeneration in CH_2Cl_2 at −60 °C. Unexpectedly, the $Ru_2^{II,III}$ arsine complexes strongly resemble the classical ruthenium 'blues' where L = NH_3 or H_2O. For such valence-delocalised systems the visible region ordinarily contains an intense $\sigma \longrightarrow \sigma^*$ band (the source of the intense blue colour) together with a much weaker, near-infrared $\delta_\pi^* \longrightarrow \sigma^*$ band. Bonding within the $\{RuX_3Ru\}^{2+}$ core can then be monitored directly by $\nu_{\sigma \longrightarrow \sigma^*}$. The distinctly different spectral appearance of the more familiar PR_3-capped mixed-valence compounds has been a long-standing puzzle, but the twenty electrogenerated 11-e binuclear systems assembled here with various AsR_3 or PR_3 terminal ligands are all delocalised, and clearly belong within a continuum of electronic behaviour with steadily decreasing metal–metal interaction. In all, $\nu_{\sigma \longrightarrow \sigma^*}$ declines over a considerable range from 17 000 to below 5000 cm^{-1}, with the ligands ranked as follows: L = NH_3 (and 1,4,7-trimethyl-1,4,7-triazacyclononane) > H_2O > Cl, Br (*i.e.* nonahalides) > AsR_3 > PR_3 and μ-Cl > μ-Br. These changes are well correlated with systematic trends in the $g_\parallel$ and $g_\perp$ components of the axial *g* tensor, and also with the gap between the stepwise oxidation potentials which shrinks from 1.2 to 0.45 V. For the PR_3 complexes the decrease in $\nu_{\sigma \longrightarrow \sigma^*}$ is accompanied by progressive intensity transfer to the $\delta_\pi^* \longrightarrow \sigma^*$ band. The anticipated Ru · · · Ru separation is of the order of 2.9 and 3.0 Å for the mixed-valence $AsMe_3$/μ-Cl and PMe_3/μ-Cl systems respectively, markedly longer than the crystallographic value of 2.75 Å in $[(NH_3)_3Ru(\mu\text{-}Cl)_3Ru(NH_3)_3]^{2+}$. The geometric distinction between the AsR_3- and PR_3-capped dimers is an unexpected consequence of selective crowding between the substituent R groups and the $\{\mu\text{-}X_3\}$ array. The present $Ru_2^{II,III}$ systems are electronically distinct from their PR_3-containing osmium counterparts, such as $[(Et_3P)_3Os(\mu\text{-}Cl)_3Os(PEt)_3]^{2+}$, which show still greater visible/near-infrared spectral deviations.

The symmetric triply halide-bridged bioctahedral architecture **I** is a recurring structure of remarkable stability and conceptual interest in ruthenium chemistry.[1–3] Familiar examples range in formal oxidation state from $[Ru_2^{III,III}Cl_9]^{3-}$ and $[Ru_2^{III,III}Br_9]^{3-}$, which are 10-e (= d^5d^5) systems potentially embodying a single Ru–Ru σ bond,[4] through the 11-e $[Ru_2^{II,III}(\mu\text{-}X)_3(H_2O)_6]^{2+}$ and $[Ru_2^{II,III}(\mu\text{-}X)_3(NH_3)_6]^{2+}$ 'blues',[5] to closed-shell 12-e $[Ru_2^{II,II}(\mu\text{-}X)_3(PR_3)_6]^+$ complexes.[6] Furthermore, through the efficacy of low-temperature electrosynthesis, both the II,II and III,III systems can be driven to the intervening mixed-valence state, and characterised *in situ*.[7,8]

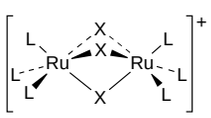

I

Here we describe the first systematic study of the structural and electronic properties of the corresponding hexakis(tertiary arsine) confacial diruthenium(II) complexes, $[(R_3As)_3Ru(\mu\text{-}X)_3Ru(AsR_3)_3]^+$ (structure **I**, where L = $AsMe_3$, $AsMe_2Ph$ or $AsMePh_2$; X = Br or Cl), and of their electrochemically derived II,III and III,III forms.[1] Quite unexpectedly, the new AsR_3-capped mixed-valence systems turn out to be sharply differentiated in optical properties from their more familiar PR_3 analogues, and closely akin to the archetypal NH_3-capped ruthenium 'blues' mentioned above. The fresh insight brought about by this discovery provides the focus for the present paper.

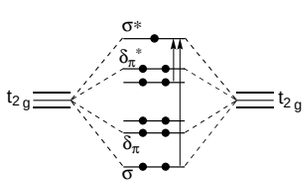

Scheme 1

The molecular-orbital diagram[9] underlying the optical behaviour of such electronically delocalised, trigonally symmetric, confacial binuclear complexes is represented in Scheme 1. As shown, a net one-electron σ bond (strictly a three-electron $\{\sigma^2\sigma^{*1}\}$ hemi-bond) prevails in the 11-e, $S = \frac{1}{2}$ ground state. For the literal 'blues', first properly and convincingly formulated by Mercer and co-workers,[5] two highly characteristic optical transitions are observed:[5,10–12] an intense *z*-polarised $\sigma \longrightarrow \sigma^*$ band near 17 000 cm^{-1} which is the source of their colour, and a weaker, *xy*-polarised $\delta_\pi^* \longrightarrow \sigma^*$ band near 7000 cm^{-1}. Owing to the odd-electron configuration and the resulting cancellation of electron-correlation terms, the observed transition energies should closely match the corresponding orbital separations. In

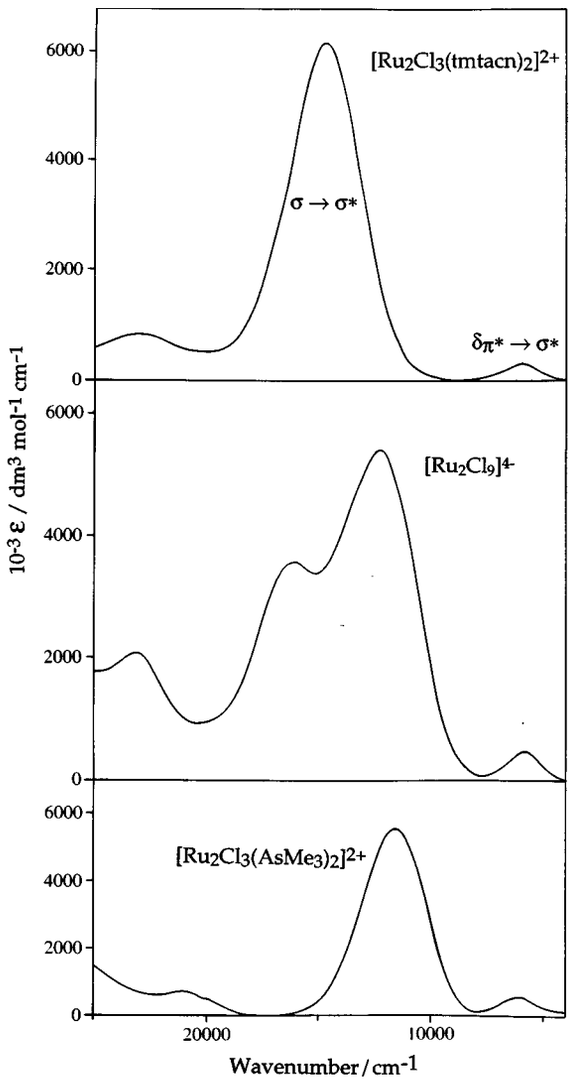

Fig. 1 Visible/near-IR band envelopes of three representative 11-e $[Ru_2(\mu\text{-}Cl)_3L_6]^z$ complexes

particular, within the limits of this theoretical model, $\nu_{\sigma\longrightarrow\sigma^*}$ can be equated with the gap between σ and σ*, equivalent to $2W_\sigma$ where W_σ is the resonance integral for the one-electron σ bond of Scheme 1.[11] Thus, the study of such confacial $Ru_2^{II,III}$ 11-e systems is exceptionally rewarding because their visible and near-infrared electronic absorption spectra directly map the underlying metal–metal bonding interactions.

Several new 1,4,7-triazacyclononane (tacn) and 1,4,7-trimethyl-1,4,7-triazacyclononane (tmtacn) NR_3-capped systems fitting this description have been developed in Wieghardt's laboratory,[13,14] and elsewhere.[15] In addition, the model was considerably widened in scope by characterisation of 11-e $[Ru_2Cl_9]^{4-}$ and $[Ru_2Br_9]^{4-}$ which, remarkably enough, reveal the same visible/near-infrared two-band profile.[8] (These electrogenerated complexes are extremely prone to halide expulsion and hydrolysis, and Kennedy and Khoo's experimental achievement[8] in identifying the $Ru_2^{II,III}$ nonahalides should be emphasised.) The new AsR_3 complexes also match the spectral pattern of classical ruthenium 'blues', as noted above. Fig. 1 shows this family resemblance, and the pronounced shift of $\nu_{\sigma\longrightarrow\sigma^*}$ to about 12 000 cm^{-1} as the capping ligands are changed from NR_3 to Cl^- and then to AsR_3.

The corresponding hexakisphosphine 11-e dications must be formed by oxidation beyond +1.0 V *vs.* the saturated calomel electrode (SCE). They were first examined by Heath and Stephenson and their colleagues[16,17] before the burgeoning interest[10–15] in ammine 'blues', and were reported in 1982 to be truly delocalised confacial $\{Ru^{2.5+}Ru^{2.5+}\}$ systems.[7] However the optical spectra of these electrogenerated PR_3-capped dications differ greatly from the archetype presented in Fig. 1. The $PMePh_2$ and $AsMePh_2$ μ-Cl complexes are directly compared in Fig. 2, and further examples are given later. The near-IR spectra of the phosphine systems are so exceptional that at times we have wondered whether the alternative, valence-trapped $\{Ru^{2+}Ru^{3+}\}$ ground state could prevail. As a counter hypothesis, this receives some support from the recent observation[18] that the isoelectronic diosmium complex $[(Et_3P)_3Os(\mu\text{-}Cl)_3Os(PEt_3)_3]^{2+}$ has a very long, arguably non-bonding, internuclear separation of 3.406(1) Å, only 0.07 Å shorter than in the $Os^{II}{}_2$ precursor.

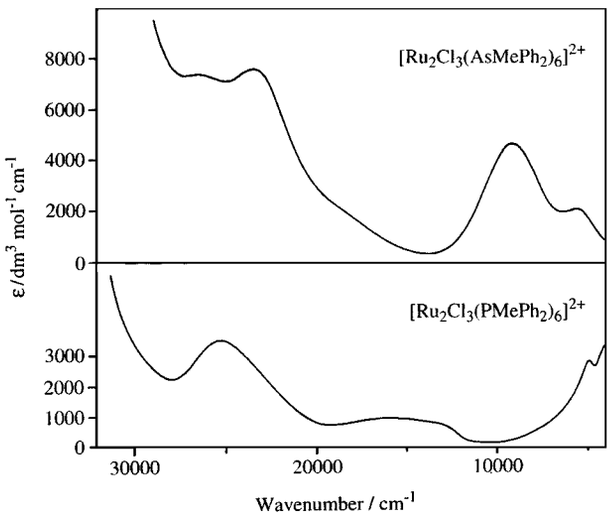

Fig. 2 Contrasting visible/near-IR spectra of $[Ru_2(\mu\text{-}Cl)_3L_6]^{2+}$ (L = $AsMe_2Ph$ or PMe_2Ph)

The unexpected optical behaviour of $AsMe_3$- and $AsMe_2Ph$-capped $Ru_2^{II,III}$ systems prompted us to characterise their PMe_3 analogues by spectroelectrochemistry for the first time. To our surprise, we discovered that, *alone among the many phosphine systems so far examined*, the $[(Me_3P)_3Ru(\mu\text{-}X)_3Ru(PMe_3)_3]^{2+}$ complexes unmistakably fit the classical spectral behaviour of Scheme 1. This paper marshalls extensive evidence, now based on detailed study of some twenty bioctahedral 11-e AsR_3 and PR_3 diruthenium compounds,[1,2] that all the phosphine complexes are delocalised despite the irregular appearance of their optical spectra. They lie within a continuum of electronic behaviour where the confacial one-electron metal–metal bond is found to diminish remarkably in strength from some 9000 cm^{-1} in the ammines to below 2500 cm^{-1} in the most weakly coupled systems characterised to date. Accordingly, this work provides the opportunity to examine the variation of metal–metal interactions in a large family of confacial $[L_3Ru(\mu\text{-}X)_3RuL_3]^{z+}$ complexes **I** as a function of donor-atom identity, substituent effects, and prevailing oxidation state.

Several of the synthetic objectives underpinning this study have proven to be non-trivial in themselves, and these issues are dealt with first in the discussion below.

Results and Discussion

The binuclear complexes under investigation are listed in Table 1. Except where noted otherwise, the accompanying counter ion is $CF_3SO_3^-$.

Synthesis

The present compounds were obtained by procedures 1–7 (AsR_3 derivatives) and 8–20 (PR_3 derivatives) detailed in the Experimental section. Since Chatt and Hayter's first recognition of $[Ru_2(\mu\text{-}Cl)_3(PR_3)_6]Cl$ complexes,[6] there have been numerous preparations of such compounds.[6,19–27] However, there are only scattered and infrequent reports[25,28,29] of the

Table 1 Electrochemical data for $[Ru_2X_3L_6]^+$ complexes

	$E_{\frac{1}{2}}$/V *vs.* Ag–AgCl[a]			
Complex	$E_{ox}(1)$	$E_{ox}(2)$	E_{av}[b]/V	$\Delta E_{\frac{1}{2}}$[c]/V
$[Ru_2Cl_3(AsMe_3)_6]^+$	+0.95	+1.63	+1.29	0.68
$[Ru_2Br_3(AsMe_3)_6]^+$	+0.95	+1.56	+1.26	0.61
$[Ru_2Cl_3(AsMe_2Ph)_6]^+$	+1.07	+1.70	+1.39	0.63
$[Ru_2Br_3(AsMe_2Ph)_6]^+$	+1.06	+1.62	+1.34	0.56
$[Ru_2Cl_3(AsMePh_2)_6]^+$	+1.19	+1.85	+1.52	0.66
$[Ru_2Br_3(AsMePh_2)_6]^+$	+1.20	+1.76	+1.48	0.56
$[Ru_2Cl_3(AsMe_3)_4(PPh_3)_2]^+$	+1.18	+1.80	+1.49	0.62
$[Ru_2Cl_3(PMe_3)_6]^+$	+1.18	+1.72	+1.45	0.54
$[Ru_2Br_3(PMe_3)_6]^+$	+1.20	+1.69	+1.45	0.49
$[Ru_2Cl_3(PMe_2Ph)_6]^+$	+1.31	+1.87	+1.59	0.56
$[Ru_2Br_3(PMe_2Ph)_6]^+$	+1.32	+1.87	+1.60	0.55
$[Ru_2Cl_3(PMePh_2)_6]^+$	+1.38	+1.92	+1.65	0.54
$[Ru_2Cl_3(PEt_3)_6]^+$	+1.09	+1.71	+1.40	0.62
$[Ru_2Br_3(PEt_3)_6]^+$	+1.11	+1.68	+1.40	0.57
$[Ru_2Cl_3(PEt_2Ph)_6]^+$	+1.19	+1.71	+1.45	0.52
$[Ru_2Br_3(PEt_2Ph)_6]^+$	+1.18	+1.70	+1.44	0.52
$[Ru_2Cl_3(PEtPh_2)_6]^+$	+1.21	+1.80[d]		
$[Ru_2Cl_3\{MeC(CH_2PPh_2)_3\}_2]^+$	+1.46	+1.94	+1.70	0.48
$[Ru_2Br_3\{MeC(CH_2PPh_2)_3\}_2]^+$	+1.47	+1.91	+1.69	0.44
$[Ru_2Cl_3\{P(OMe)Ph_2\}_6]^+$	+1.46[d]	+1.97[e]		
$[Ru_2Cl_3(tmtacn)_2]^{2+}$	−0.09	+1.10	+0.51	1.19
$[Ru_2Br_3(tmtacn)_2]^{2+}$	+0.04	+1.09	+0.57	1.05
$[Os_2Cl_3(PMe_2Ph)_6]^+$	+1.07	+1.57	+1.32	0.50
$[Os_2Br_3(PMe_2Ph)_6]^+$	+1.05	+1.55	+1.30	0.50

[a] Recorded in CH_2Cl_2 containing 0.5 mol dm^{-3} $[NBu^n_4][BF_4]$ at 213 K; ferrocene is oxidised at +0.55 V *vs.* Ag–AgCl under these conditions. [b] $E_{av} = \frac{1}{2}[E_{ox}(1) + E_{ox}(2)]$. [c] $\Delta E_{\frac{1}{2}} = E_{ox}(2) - E_{ox}(1)$. [d] Quasi-reversible. [e] Irreversible.

analogous tertiary arsine complexes. Reddy and co-workers[28,29] obtained the series $[Ru_2Cl_3(AsRPh_2)_6]Cl$ (R = Me, Et, Pr^n or Bu^n), but in a manner seemingly specific to alkyldiphenylarsine derivatives. This involved heating $RuCl_3 \cdot xH_2O$ in ethanol in the presence of $AsRPh_2$, as in the original synthesis[6] of $[Ru_2Cl_3(PR_3)_6]Cl$. Our attempts to prepare the corresponding $AsMe_3$ and $AsMe_2Ph$ binuclear complexes under similar conditions gave *trans*-$[RuCl_2(AsR_3)_4]$ instead. Neutral phosphine complexes of the form $[RuCl_2(PR_3)_n]$ (n = 3 or 4) are known to condense spontaneously to $[Ru_2Cl_3(PR_3)_6]Cl$ in polar solvents,[21] and *trans*-$[RuCl_2(AsMePh_2)_4]$ dimerises in the same fashion when warmed in ethanol with a small amount of $AsMePh_2$.[29] In contrast, we have established that neither *trans*-$[RuCl_2(AsMe_3)_4]$ nor *trans*-$[RuCl_2(AsMe_2Ph)_4]$ transforms to $[Ru_2Cl_3(AsR_3)_6]^+$ under these mild conditions, and this sheds some light on the failure of Reddy's method in the more general case.

Given the variable composition of $RuCl_3 \cdot xH_2O$, we turned to stoichiometric, tervalent $K_3[Ru_2Cl_9]$ as an advantageous starting material.[30] In absolute ethanol, the product of the reaction of $K_3[Ru_2Cl_9]$ with AsR_3 was again *trans*-$[RuCl_2(AsR_3)_4]$, however deliberate inclusion of water (water : EtOH 1 : 4) led to formation of a measurable proportion of $[Ru_2Cl_2(AsR_3)_6]Cl$. Emergence of the ionic product is possibly attributable to the increase in solvent polarity. The accompanying *trans*-$[Ru_2Cl_2(AsR_3)_4]$ compounds tend to precipitate from the reaction mixture, conveniently leaving $[Ru_2Cl_3(AsR_3)_6]Cl$ in solution. Upon work-up this method gave moderate yields of $[Ru_2Cl_3(AsR_3)_6]Cl$ complexes for $AsR_3 = AsMe_3$, $AsMe_2Ph$ and $AsMePh_2$. (On reinvestigation, reactions of $RuCl_3 \cdot xH_2O$ in water–ethanol mixtures also gave the binuclear product, but always in lower yield.) In addition, the bromide-bridged analogues $[Ru_2Br_3(AsR_3)_6]Br$, which had not been reported at all before, can be prepared from $K_3[Ru_2Br_9]$[30,31] by equivalent procedures.

The products were routinely converted into the corresponding redox-inert $CF_3SO_3^-$ salts. This was achieved by gently heating CH_2Cl_2 solutions of $[Ru_2X_3(AsR_3)_6]X$ in the presence of CF_3SO_3H to release HX. After evaporation of the solvent, each solid residue was readily recovered from CH_2Cl_2–Et_2O as yellow crystalline $[Ru_2(\mu\text{-}X)_3(AsR_3)_6][CF_3SO_3]$.

At an earlier stage we had attempted to synthesize $[Ru_2Cl_3(AsR_3)_6]Cl$ complexes starting from $[RuCl_2(PPh_3)_3]$. A similar procedure has been widely used to prepare $[Ru_2Cl_3(PR_3)_6]Cl$ complexes in good quantity, through the ready displacement of PPh_3. Extended heating of an ethanol mixture of $[RuCl_2(PPh_3)_3]$ and $AsMe_3$ gave a yellow product of precise stoichiometry $[Ru_2Cl_3(AsMe_3)_4(PPh_3)_2][CF_3SO_3]$, after treatment with CF_3SO_3H and normal work-up. Several isomers are possible. However, the $^{31}P\text{-}\{^1H\}$ NMR spectrum revealed a single peak at δ +53.2, whilst the ^1H NMR (an aryl multiplet and singlets at δ 0.66 and 1.16) corresponded to distinguishable PPh_3 and $AsMe_3$ ligands in the ratio 1 : 1 : 1. This suggests the exclusive presence of an evenly ligated binuclear complex, $[(Ph_3P)(Me_3As)_2Ru(\mu\text{-}Cl)_3Ru(AsMe_3)_2(PPh_3)]^+$, with PPh_3 ligands staggered as shown in structure **II**. Attempts to displace the remaining PPh_3 by prolonged heating with an excess of $AsMe_3$ gave no evidence of further substitution.

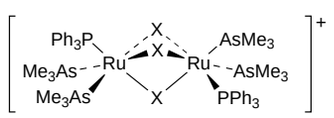

II

In contrast to the arsine-capped systems, the $[Ru_2Cl_3(PR_3)_6]^+$ complexes investigated in the course of this work (see Table 1) have all been prepared previously, in a variety of ways. We re-examined these procedures in an attempt to define a reliable general synthesis. In most cases, adaptation of Stephenson's methods[21,23] provided a convenient route to the chloride salts. This involves boiling absolute ethanol suspensions of $[RuCl_2(PPh_3)_3]$ and the appropriate phosphine for an extended period. Alternative solvents proved more effective in the case of $[Ru_2Cl_3\{MeC(CH_2PPh_2)_3\}_2]Cl$ (2-methoxyethanol) and $[Ru_2Cl_3\{P(OMe)Ph_2\}_6]Cl$ (methanol). The former complex and its arsenic analogue were originally obtained by heating *cis*-$[RuCl_2(dmso)_4]$ (dmso = dimethyl sulfoxide) and the ligand in

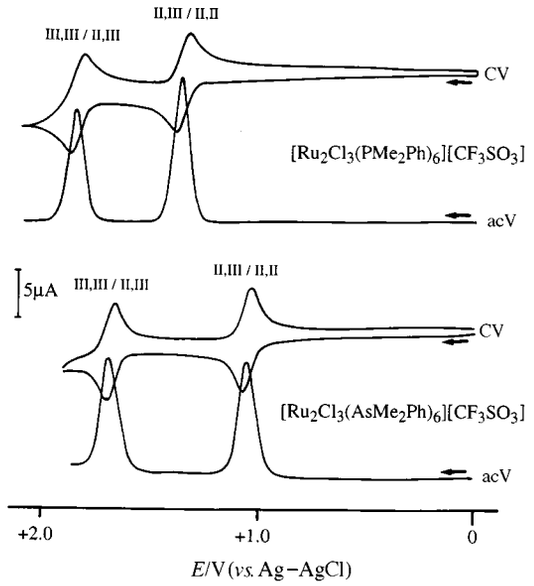

Fig. 3 Cyclic (CV) and a.c. voltammetry (acV) of $[Ru_2(\mu\text{-}Cl)_3L_6][CF_3SO_3]$ (L = PMe_2Ph or $AsMe_2Ph$)

toluene.[25] It should be noted that carbonylation frequently accompanies ligand substitution when 2-methoxyethanol is employed for reaction of monodentate phosphines with $[RuCl_2(PPh_3)_3]$, leading, for example, to the isolation of known *cis*-$[RuCl_2(CO)(PR_3)_3]$ complexes.[32]

Bromide-bridged $[Ru_2Br_3(PR_3)_6]^+$ complexes are far less common in the literature than their chloride analogues. An early preparation of $[Ru_2Br_3(PMe_2Ph)_6]^+$, from $RuCl_3{\cdot}xH_2O$, PMe_2Ph and excess of LiBr,[19] was later shown to yield a mixture of all four $[Ru_2(\mu\text{-}Cl)_x(\mu\text{-}Br)_{3-x}(PMe_2Ph)_6]^+$ complexes ($x = 0$–3), and the authentic compound was ultimately prepared from $[RuBr_2(PPh_3)_3]$.[33] In the present work, both $[Ru_2Br_3(PMe_2Ph)_6]^+$ and $[Ru_2Br_3(PEt_3)_6]^+$ were prepared by heating $[RuBr_2(PPh_3)_3]$ with an excess of phosphine in ethanol, and $[Ru_2Br_3\{MeC(CH_2PPh_2)_3\}_2]^+$ was prepared similarly in 2-methoxyethanol.

Two complexes in particular, $[Ru_2Cl_3(PMePh_2)_6]Cl$ and $[Ru_2Br_3(PEt_2Ph)_6]Br$, were obtained only in poor yield and purity from $[RuX_2(PPh_3)_3]$ (X = Cl or Br), possibly due to competition between PR_3 and PPh_3. Better yields of the pure products were achieved by heating $K_3[Ru_2X_9]$ with the appropriate phosphine in ethanol. The vitally important PMe_3 derivatives (see Introduction) could not be prepared at all by the $[RuX_2(PPh_3)_3]$ route, whereas the $K_3[Ru_2X_9]$ route succeeded. Reaction of $[RuX_2(PPh_3)_3]$ and PMe_3 in ethanol gave only *trans*-$[RuX_2(PMe_3)_4]$. As with their $AsMe_3$ analogues, these neutral monomers resisted condensation to the triply bridged structure. However, $[Ru_2Cl_3(PMe_3)_6][CF_3SO_3]$ and $[Ru_2Br_3(PMe_3)_6][CF_3SO_3]$ were readily prepared by reaction of PMe_3 in aqueous ethanol with $K_3[Ru_2Cl_9]$ or $K_3[Ru_2Br_9]$ as appropriate, and CF_3SO_3H metathesis in the usual way.

Electrochemistry

This paper provides the first account of the voltammetric response of the hexakis(arsine) complexes. In company with their phosphine-capped predecessors,[7] they display two handsome reversible oxidations as illustrated in Fig. 3. Bulk coulometry for the first step and steady-state voltammetry employing a rotating platinum electrode establish that both steps are one-electron processes, in accord with Scheme 2. The electrogenerated $\{Ru_2^{III,III}\}^{3+}$ ions are very reactive and tend to degrade in an undetermined way at room temperature. Accordingly, the electrode potentials for all compounds listed in Table 1 have been measured at −60 °C. Under these conditions there is conclusive spectroelectrochemical evidence that all the singly oxidised species and some of the doubly oxidised species can

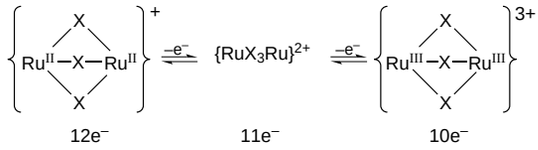

Scheme 2

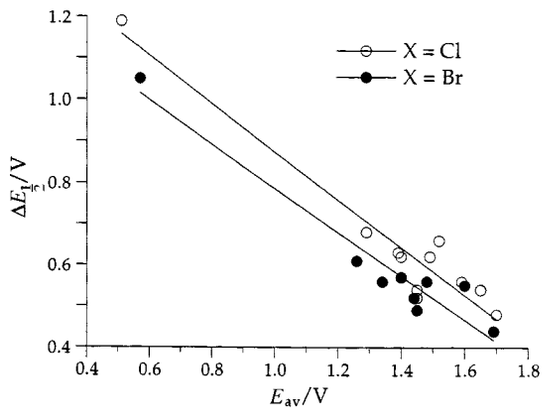

Fig. 4 Correlation of $\Delta E_{\frac{1}{2}}$ with E_{av} for the twenty $[Ru_2(\mu\text{-}X)_3L_6]^+$ complexes of Table 1

persist unchanged in solution for several hours in the presence of a suitably polarised electrode (see below).

At first sight, there is little in Table 1 or Fig. 3 to suggest a distinction in electronic properties between the arsine and phosphine dimers that might explain the marked contrast in their near-infrared spectra.

Rather than focusing on the individual couples, it is important to consider their *mean*, E_{av} [$= \frac{1}{2}(E_1 + E_2)$], and their *separation*, $\Delta E_{\frac{1}{2}}$ [$= (E_2 - E_1)$], since the separation varies significantly from one complex to another. For example, for the tmtacn/μ-Cl dimer $E_{av} = +0.5$ V and $\Delta E_{\frac{1}{2}}$ is exceptionally large at 1.2 V, while for the $AsMe_3$/μ-Cl dimer $E_{av} = +1.3$ V but $\Delta E_{\frac{1}{2}}$ is only 0.7 V. This means that the underlying shift in E_{av} between the two complexes is 0.8 V, as distinct from the shifts of 1.0 and 0.5 V exhibited by E_1 and E_2 respectively.

Considered in this way, the electrochemical data in Table 1 permit a number of empirical generalisations. (*i*) Within either the AsR_3 or the PR_3 series, variation in R (mainly substituting aryl for alkyl) is capable of shifting couples by up to 0.25 V. (*ii*) Compared to their exact PR_3 congeners, the six AsR_3 dimers are characteristically easier to oxidise by about 0.2 V (the mean shift in E_{av} is 190 mV), and they display a distinctly greater separation (mean difference in $\Delta E_{\frac{1}{2}} = 90$ mV). (*iii*) Closer analysis of the $[Ru_2X_3(AsR_3)_6]^+$ data shows that the μ-Br dimers tend to have smaller $\Delta E_{\frac{1}{2}}$ values than their μ-Cl analogues (by ≈70 mV) and to be collectively easier to oxidise, with E_{av} shifting by 40 mV. (*iv*) In contrast, in the PR_3 analogues, $\Delta E_{\frac{1}{2}}$ contracts by only ≈30 mV on average when μ-Br replaces μ-Cl, while E_{av} shifts by a marginal 5 mV. (*v*) The mixed-ligand complex $[Ru_2Cl_3(AsMe_3)_4(PPh_3)_2]^+$ is unexceptional in its redox properties; inclusion of one PPh_3 ligand in place of $AsMe_3$ on each Ru leads to an increase by 200 mV in E_{av} (largely the effect of the Ph groups), and a decrease of 60 mV in $\Delta E_{\frac{1}{2}}$.

These small differences have been pursued in detail because of circumstantial evidence (to be discussed overleaf) that they determine the nature of mixed valency in the Ru_2 systems. Fig. 4 shows clearly that the E_{av} and $\Delta E_{\frac{1}{2}}$ terms are mutually correlated (once chloro and bromo families are separated), despite natural experimental scatter among the data for the more closely related compounds.† We note in passing that the

† We have not revisited these data, collected over some 6 years, to pursue small 'discrepancies' suggested by the current analysis.

Table 2 The UV/VIS/near-IR spectral data for $[Ru_2X_3L_6]^+$ complexes

Complex	$\tilde{\nu}_{max}$/cm^{-1} (ε/dm^3 mol^{-1} cm^{-1})*
$[Ru_2Cl_3(AsMe_3)_6][CF_3SO_3]$	25 090 (1030), 29 000 (950), 35 700 (3830)
$[Ru_2Br_3(AsMe_3)_6][CF_3SO_3]$	24 300 (1460), 28 000 (740), 34 000 (5200), 40 800 (32 900)
$[Ru_2Cl_3(AsMe_2Ph)_6][CF_3SO_3]$	24 000 (2960), 27 560 (3940), 33 720 (9550), 41 630 (78 200)
$[Ru_2Br_3(AsMe_2Ph)_6][CF_3SO_3]$	23 100 (2490), 26 600 (3270), 32 200 (6390), 38 500 (sh), 40 900 (56 600)
$[Ru_2Cl_3(AsMePh_2)_6][CF_3SO_3]$	23 400 (1010), 26 600 (1370), 32 320 (4550), 40 450 (43 400)
$[Ru_2Br_3(AsMePh_2)_6][CF_3SO_3]$	22 500 (2020), 31 000 (3460), 40 100 (42 100)
$[Ru_2Cl_3(AsMe_3)_4(PPh_3)_2][CF_3SO_3]$	24 760 (2500), 33 630 (8150)
$[Ru_2Cl_3(PMe_3)_6][CF_3SO_3]$	28 900 (1710), 31 900 (1520), 38 970 (3570)
$[Ru_2Br_3(PMe_3)_6][CF_3SO_3]$	28 000 (1430), 36 710 (2690), 43 250 (20 800)
$[Ru_2Cl_3(PMe_2Ph)_6][CF_3SO_3]$	29 450 (3730)
$[Ru_2Br_3(PMe_2Ph)_6][CF_3SO_3]$	28 520 (3740)
$[Ru_2Cl_3(PMePh_2)_6][CF_3SO_3]$	25 200 (2150), 27 550 (2680), 32 950 (4870)
$[Ru_2Cl_3(PEt_3)_6][CF_3SO_3]$	27 150 (1740), 30 270 (2290), 36 230 (5460)
$[Ru_2Br_3(PEt_3)_6][CF_3SO_3]$	26 180 (2100), 29 380 (2800), 34 380 (5440)
$[Ru_2Cl_3(PEt_2Ph)_6][CF_3SO_3]$	28 800 (3130), 34 300 (6340)
$[Ru_2Br_3(PEt_2Ph)_6][CF_3SO_3]$	28 490 (3300), 33 380 (6090), 41 320 (98 600)
$[Ru_2Cl_3(PEtPh_2)_6][CF_3SO_3]$	27 440 (3180)
$[Ru_2Cl_3\{MeC(CH_2PPh_2)_3\}_2][CF_3SO_3]$	27 230 (6020)
$[Ru_2Br_3\{MeC(CH_2PPh_2)_3\}_2][CF_3SO_3]$	26 100 (6320)
$[Ru_2Cl_3\{P(OMe)Ph_2\}_6][CF_3SO_3]$	27 810 (4430)

* Recorded in CH_2Cl_2 containing 0.5 mol dm^{-3} $[NBu^n_4][BF_4]$ at 213 K.

diosmium PMe_2Ph systems included in Table 1 are roughly 0.3 V easier to oxidise than their Ru_2 congeners but, unexpectedly and perhaps significantly, have $\Delta E_{\frac{1}{2}}$ values some 50 mV *smaller* (see Conclusion).

The voltammetric data included here for the tmtacn systems, measured in our laboratory under the same conditions (Table 1), reveal characteristically large values for $\Delta E_{\frac{1}{2}}$, which agree with those reported by Wieghardt's group for these compounds in MeCN at room temperature.[14] Recently, in connection with a remarkable Ru^{III}-catalysed four-electron reduction of O_2, Shi and Anson[34] described the well defined reduction of $[Ru_2Cl_3(NH_3)_6]^{2+}$ in 0.1 mol dm^{-3} aqueous CF_3CO_2H. In this situation the electrogenerated $Ru_2^{II,II}$ species cleaves on the cyclic voltammetric time-scale, and the gap between the successive III,III ⟶ II,III and II,III ⟶ II,II waves decreases to ≈0.9 V. We have established that blue, organo-soluble $[Ru_2Cl_3(NH_3)_6]BPh_4$ in chilled MeCN reveals a reversible oxidation *and* a reversible reduction, separated by 1.23 V.

Spectroelectrochemistry

***(i)* General features of the optical spectra.** As ordinarily isolated, the complexes $[(R_3As)_3Ru(\mu\text{-}X)_3Ru(AsR_3)_3]^+$ and their PR_3 analogues exist in the relatively uninformative closed-shell oxidation state, in contrast to the archetypal ruthenium ammine 'blues' which are found naturally in the II,III form. Optical spectroelectrochemistry plays a key role in this work; firstly, because it gives access to all the mixed-valence $[L_3Ru(\mu\text{-}X)_3RuL_3]^{2+}$ species and establishes their individual stability, and, secondly, because near-infrared spectroscopy is the first-choice probe of electronic behaviour for such systems. The optical data (45 000 to 3125 cm^{-1}) for successive II,II, II,III and III,III states are collected in Tables 2, 3 and 4, respectively.

Fig. 5 shows the stepwise electro-oxidation of $[Ru_2Cl_3(AsMe_2Ph)_6]^+$ monitored in an optical semi-thin-layer electrochemical (OSTLE) cell at low temperature, with typical time-dependent progressions to the successive II,III and III,III states. A separate family of isosbestic points prevails for each step. Three strict requirements in the present work for inclusion in Tables 3 and 4 are: integrity of all isosbestic points, checks for complete electrolysis at each stage, and full retrieval of the starting spectrum upon electrochemical regeneration. The limiting traces for the three successive oxidation states $[Ru_2Cl_3(AsMe_2Ph)_6]^{z+}$ (z = 1, 2, 3) are overlaid in the lower panel of Fig. 5.

All the $Ru_2^{II,II}$ compounds listed in Table 2 show an intense absorption near 40 000 cm^{-1}, presumably associated with

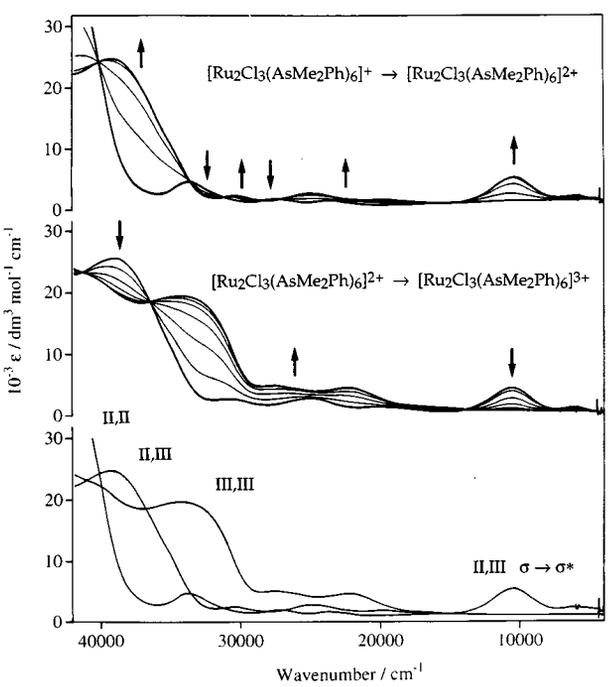

Fig. 5 The UV/near-IR spectral progressions upon oxidation of $[Ru_2(\mu\text{-}Cl)_3(AsMe_2Ph)_6]^+$ and $[Ru_2(\mu\text{-}Cl)_3(AsMe_2Ph)_6]^{2+}$ in a thin-layer cell. Limiting traces for the II,II, II,III and III,III states are superimposed in the lower panel

L(σ)→Ru charge transfer from AsR_3 or PR_3 (where the acceptor level is related to the local e_g orbital of a single metal ion). This assignment is indicated by the resemblance between the chloro and bromo derivatives (see below). The strong ligand-to-metal charge-transfer bands persist in red-shifted form for the II,III and III,III states. The II,II dimers are featureless throughout the visible/near-IR range, and particularly transparent below ≈15 000 cm^{-1} (ε < 100 dm^3 mol^{-1} cm^{-1}), which aids the definition of the emerging near-infrared bands for the II,III state. Upon further oxidation these bands collapse again, which confirms they are peculiar to the 11-e configuration rather than being characteristic single-ion (Ru^{3+}) features. This holds true for the PR_3 compounds as well, despite the additional complexities in their near-IR spectra mentioned above.

A distinctive aspect of the II,III and III,III spectra is the similarity of the μ-Cl and μ-Br systems throughout the UV/VIS

Table 3 The UV/VIS/near-IR spectral data for $[Ru_2X_3L_6]^{2+}$ complexes

Complex	$\tilde{\nu}_{max}$/cm^{-1} (ε/dm^3 mol^{-1} cm^{-1})*		
	$\delta_\pi^* \longrightarrow \sigma^*$	$\sigma \longrightarrow \sigma^*$	Other bands
$[Ru_2Cl_3(AsMe_3)_6]^{2+}$	6 400 (720)	11 800 (5600)	21 200 (720), 27 700 (2300), 31 500 (1240)
$[Ru_2Br_3(AsMe_3)_6]^{2+}$	6 470 (1130)	11 150 (6600)	19 700 (540), 25 100 (1890), 27 100 (2480), 31 000 (2030)
$[Ru_2Cl_3(AsMe_2Ph)_6]^{2+}$	6 250 (2140)	10 510 (8680)	20 000 (2800), 25 100 (5520), 30 600 (5050), 38 970 (48 100)
$[Ru_2Br_3(AsMe_2Ph)_6]^{2+}$	5 900 (1800)	10 100 (4800)	23 900 (3970), 20 000 (sh), 37 900 (43 100)
$[Ru_2Cl_3(AsMePh_2)_6]^{2+}$	6 200 (1930)	9 700 (4580)	23 740 (7500), 26 500 (7230), 37 040 (29 000)
$[Ru_2Br_3(AsMePh_2)_6]^{2+}$	5 800 (2020)	8 700 (3170)	20 100 (1730), 22 200 (2890), 36 900 (33 200)
$[Ru_2Cl_3(AsMe_3)_4(PPh_3)_2]^{2+}$	4 900 (2630)	8 600 (5290)	25 100 (4370)
$[Ru_2Cl_3(PMe_3)_6]^{2+}$	5 800 (2360)	9 350 (7500)	19 660 (220), 24 200 (sh), 28 490 (2510), 33 800 (1540)
$[Ru_2Br_3(PMe_3)_6]^{2+}$	5 590 (2430)	8 870 (5080)	16 600 (150), 23 100 (sh), 27 060 (2220), 31 900 (1630)
$[Ru_2Cl_3(PMe_2Ph)_6]^{2+}$	5 100 (2390)	7 950 (3330)	17 000 (730), 28 000 (4400)
$[Ru_2Br_3(PMe_2Ph)_6]^{2+}$	4 700 (3440)	7 400 (2480)	17 600 (950), 26 800 (4660)
$[Ru_2Cl_3(PMePh_2)_6]^{2+}$	4 050 (3300)	4 950 (2780)	15 930 (930), 25 200 (3480)
$[Ru_2Cl_3(PEt_3)_6]^{2+}$	4 600 (3000)	7 460 (2580)	16 500 (350), 27 000 (3830)
$[Ru_2Br_3(PEt_3)_6]^{2+}$	4 140 (4200)	6 500 (1600)	14 230 (420), 26 020 (4350)
$[Ru_2Cl_3(PEt_2Ph)_6]^{2+}$	4 500 (2800)	6 250 (1500)	16 900 (720), 25 960 (3510)
$[Ru_2Br_3(PEt_2Ph)_6]^{2+}$	4 100 (3980)	4 700 (sh)	13 100 (720), 16 800 (990), 25 600 (3900)
$[Ru_2Cl_3(PEtPh_2)_6]^{2+}$	4 900 (2700)	6 980 (1610)	16 920 (990), 24 100 (3140)
$[Ru_2Cl_3\{MeC(CH_2PPh_2)_3\}_2]^{2+}$	4 100 (1580)	5 300 (1700)	17 000 (800), 27 460 (6200)
$[Ru_2Br_3\{MeC(CH_2PPh_2)_3\}_2]^{2+}$	4 360 (3140)	5 400 (3000)	22 800 (14 000)
$[Ru_2Cl_3\{P(OMe)Ph_2\}_6]^{2+}$	4 900 (1720)	8 420 (1760)	14 740 (920), 27 270 (4100)

* Recorded in CH_2Cl_2 containing 0.5 mol dm^{-3} $[NBu^n_4][BF_4]$ at 213 K. Spectra were obtained by *in situ* electrogeneration as described in the text.

Table 4 The UV/VIS/near-IR spectral data for $[Ru_2X_3L_6]^{3+}$ complexes

Complex	$\tilde{\nu}_{max}$/cm^{-1} (ε/dm^3 mol^{-1} cm^{-1})
$[Ru_2Cl_3(AsMe_2Ph)_6]^{3+}$	22 370 (8600), 27 600 (9300), 33 900 (37 600)
$[Ru_2Br_3(AsMe_2Ph)_6]^{3+}$	21 700 (4300), 24 600 (4600), 33 000 (31 900), 42 700 (46 600)
$[Ru_2Cl_3(AsMePh_2)_6]^{3+}$	22 000 (7290), 27 900 (8860), 32 960 (45 000), 39 340 (37 400)
$[Ru_2Cl_3(PEt_3)_6]^{3+}$	**11 100** (**4550**), 16 200 (1100), 25 480 (3540), 27 800 (3540)
$[Ru_2Br_3(PEt_3)_6]^{3+}$	4 200 (300), **10 090** (**3110**), 16 800 (2340)
$[Ru_2Cl_3(PEt_2Ph)_6]^{3+}$	4 500 (170), **10 100** (**3850**), 12 600 (1800)
$[Ru_2Br_3(PEt_2Ph)_6]^{3+}$	9 800 (5150), **12 500** (**2570**), 34 410 (60 100)

* Recorded in CH_2Cl_2 containing 0.5 mol dm^{-3} $[NBu^n_4][BF_4]$ at 213 K. Spectra were obtained by *in situ* electrogeneration. The suggested pairwise transition (see text) in PR_3 complexes is shown in bold.

region. One might have anticipated obvious features associated with $X \rightarrow Ru^{III}$ charge transfer, red-shifted by 6000 cm^{-1} or so for the bromo complex. The unexpected spectral convergence between chloro and bromo analogues is also seen for the corresponding μ-Cl and μ-Br hexaammines; it turns out to have a cogent topological explanation based on the inability of the bridging halide ligands to participate effectively in charge transfer to the trigonally organised lowest-lying metal acceptor orbital.[4]

For the III,III complexes the relatively high single-ion 10*Dq* value for Ru^{3+} should displace the 'ligand-field' transitions to above 25 000 cm^{-1}. Coupled with the absence of early XMCT absorption, noted above, this means that the near-UV/VIS spectrum is dominated by the $\sigma \longrightarrow \sigma^*$ and $\delta_\pi^* \longrightarrow \sigma^*$ transitions within the binuclear manifold, uncomplicated by other features. These highly oxidised d^5d^5 complexes raise many technical issues,[4] which will be discussed in a separate paper. For the present, we note only that, while the PR_3-capped III,III complexes have a remarkable, intense feature near 10 000 cm^{-1} (Table 4), the isoelectronic hexaarsine complexes have orthodox visible/near-IR spectra much as measured previously[2,4] for their ammine counterparts. The well defined absorption near 22 000 cm^{-1} (Fig. 5) is provisionally assigned to the $Ru_2^{II,III}$ $\sigma \longrightarrow \sigma^*$ band. In even-electron (10-e) systems this transition is expected to be strongly disturbed by correlation effects which cause the band to be displaced to higher energy by as much as 10 000 cm^{-1} relative to the underlying σ–σ* orbital separation.[4]

***(ii)* Near-IR spectra of $Ru_2^{II,III}$ systems.** We now turn to closer examination of the near-IR spectra, which are of primary importance because of their direct bearing on metal–metal bonding in the mixed-valence $[L_3Ru(\mu\text{-}X)_3RuL_3]^{2+}$ state. Fig. 6 shows how the arsine-capped dimers (L = $AsMe_3$ or $AsMe_2Ph$, X = Cl or Br) all share the classical band envelope of the established 'blues', despite the $\sigma \longrightarrow \sigma^*$ band being shifted to substantially lower energies (between 12 000 and 10 000 cm^{-1}). The mixed-ligand $\{(AsMe_3)_2(PPh_3)\}$-capped chromophore falls clearly into the same category, resembling most closely the Br/$AsMePh_2$ system of Fig. 6.

The spectral envelopes for the fully phosphine-capped complexes are much more varied. Fig. 7 reveals that, among the many hexakis(phosphine) complexes we have characterised, *only the PMe_3 derivatives lend a classical appearance to the $Ru_2^{II,III}$ near-IR spectrum*. With the benefit of these new examples (L = PMe_3, X = Cl or Br), it can clearly be seen that the phosphine systems form a series in which the near-infrared spectra still contain discernible $\sigma \longrightarrow \sigma^*$ and $\delta_\pi^* \longrightarrow \sigma^*$ components but become progressively less orthodox in appearance as the manifold shifts ever lower in energy. The anomaly then rests in the dramatic intensity transfer between the two bands as they begin to converge. An alternative reading in which the two bands cross over, so that $\sigma \longrightarrow \sigma^*$ retains the greater intensity, can be dismissed on several grounds (see later).

In the original investigation of a wider family of confacial mixed-valence chromophores, $[(R_3P)_{3-x}Cl_xRu(\mu\text{-}Cl)_3RuCl_y(PR_3)_{3-y}]^{2-x-y}$, the fully symmetric (*i.e.* $x = y$) systems were reported to display a second characteristic band, at higher energy, in addition to the weak low-energy intervalence charge-transfer absorption now recognised as the $\delta_\pi^* \longrightarrow \sigma^*$ band. The movement of the higher band appeared to parallel the degree of interaction between the two metal centres.[7] This rather tentative conclusion turns out to have been a fairly apt

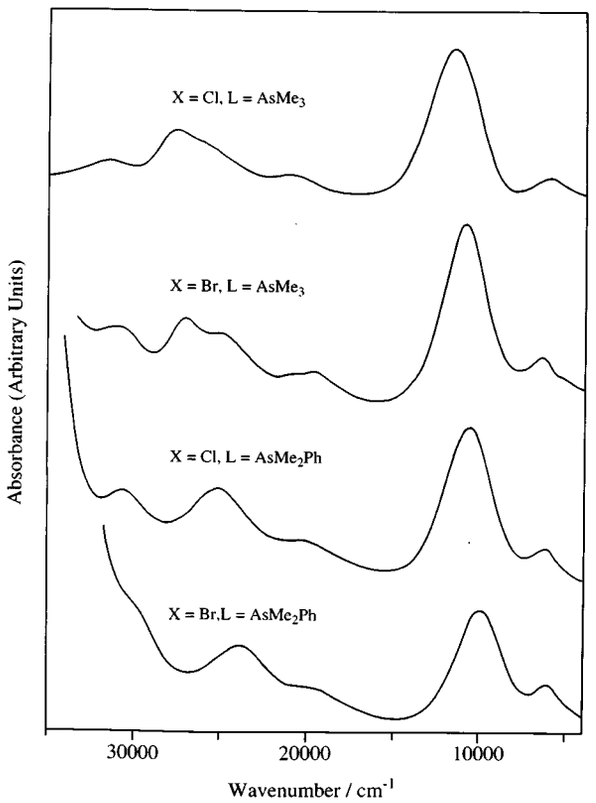

Fig. 6 Trends in electronic spectra for $[Ru_2(\mu\text{-}X)_3(AsR_3)_6]^{2+}$ complexes (X = Cl or Br)

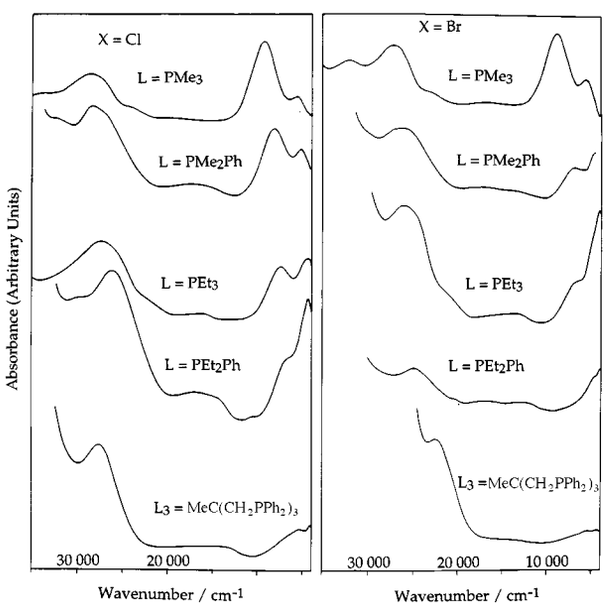

Fig. 7 Trends in electronic spectra for $[Ru_2(\mu\text{-}X)_3(PR_3)_6]^{2+}$ complexes (X = Cl or Br)

description of the $\sigma \longrightarrow \sigma^*$ band of $[(R_3P)_3Ru(\mu\text{-}Cl)_3Ru(PR_3)_3]^{2+}$ and related complexes.

The EPR data described in the next section offer strong supporting evidence that the present AsR_3 and PR_3 complexes collectively represent a continuum of delocalised 11-e electronic structures. We conclude that the non-classical appearance of some of the near-IR spectra is a consequence of complexities in optical behaviour in the limit of ever-diminishing confacial σ–σ^* splitting and not due to a dichotomy in Ru–Ru bonding in the ground state. A more comprehensive treatment[35] reveals that the simple picture conveyed by the molecular-orbital diagram of Scheme 1 (*i.e.* a strong $\sigma \longrightarrow \sigma^*$ band and a less intense $\delta_\pi^* \longrightarrow \sigma^*$ band, with $\nu_{\delta_\pi^* \longrightarrow \sigma^*}$ somewhat less than

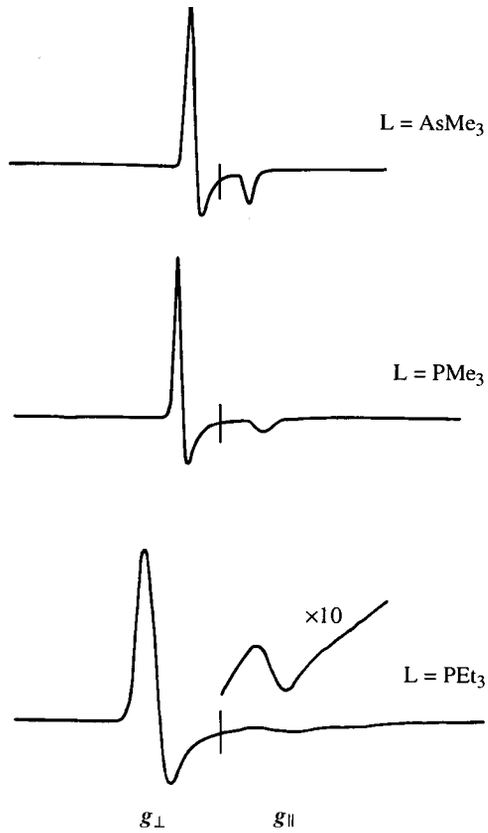

Fig. 8 The EPR spectra of $[Ru_2(\mu\text{-}Cl)_3L_6]^{2+}$ complexes (L = $AsMe_3$, PMe_3 or PEt_3). The datum line represents a g value of 2.00

half $\nu_{\sigma \longrightarrow \sigma^*}$) is bound to break down in the domain of weaker, but still delocalised, metal–metal coupling which prevails in the phosphine systems. In brief, as the energy of the $\sigma \longrightarrow \sigma^*$ transition diminishes markedly and the $\sigma \longrightarrow \sigma^*$ and $\delta_\pi^* \longrightarrow \sigma^*$ bands begin to converge, metal-centred spin–orbit coupling promotes an intensity-transfer mechanism and this is the origin of the progressively distorted near-IR manifolds in Fig. 7. An important corollary is that the higher maximum retains its significance as $\nu_{\sigma \longrightarrow \sigma^*}$ throughout the series, despite the changing appearance of the near-IR manifold.

This means that in the present study it is possible to rank the orderly progress of the crucial $\sigma \longrightarrow \sigma^*$ band over a body of more than twenty $Ru_2^{II,III}$ complexes (including the ammines). To a good approximation, the frequency of this band in the 11-e state is equal to $2W_\sigma$, where W_σ is the resonance energy associated with the one-electron ($\sigma^2\sigma^{*1}$) bond. Thus the $\sigma \longrightarrow \sigma^*$ band provides a linear measure of metal–metal coupling, including both direct and bridge-mediated contributions. An apparently logical correlation between the electrochemical and optical data is observed, such that those binuclear compounds which are relatively electron-deficient and less closely coupled (higher E_{av} and smaller ΔE_2) are precisely the ones to have lower $\sigma \longrightarrow \sigma^*$ promotion energies. Closer analysis is deferred until the corresponding EPR data for the same 11-e systems have been presented.

***(iii)* EPR Spectra of $Ru_2^{II,III}$ systems.** Hitherto, reports of EPR spectra of triply halide-bridged $Ru_2^{II,III}$ systems have been rather scattered, and no particular significance has been attached to them except to establish the paramagnetic nature and overall symmetry of the complexes in question. Only compounds naturally isolated in the II,III state have been examined elsewhere,[36,37] apart from early electrogenerative studies on the series $[L_{3-x}Cl_xRu(\mu\text{-}Cl)_3RuCl_yL_{3-y}]^{2-x-y}$ (L = mainly PR_3 or AsR_3), where the total number of terminal chloride ligands ($x + y$) ranged from 0 to 3.[7]

Fig. 8 illustrates the range of EPR behaviour spanned by

Table 5 The EPR data for $[Ru_2X_3L_6]^{2+}$ complexes

Complex	$\tilde{\nu}_{\sigma\longrightarrow\sigma^*}$ [a]/cm^{-1}	EPR [b] $g_\perp$	EPR [b] $g_\parallel$
$[Ru_2Cl_3(NH_3)_6]^{2+}$ [c]	17 100	2.10	1.95
$[Ru_2Br_3(NH_3)_6]^{2+}$ [c]	15 700	2.16	1.95
$[Ru_2Cl_3(tmtacn)_6]^{2+}$ [d]	14 700	2.12	1.90
$[Ru_2Br_3(tmtacn)_6]^{2+}$ [d]	13 240	2.23	2.03
$[Ru_2Cl_3(H_2O)_6]^{2+}$ [e]	16 500	2.08	1.96
$[Ru_2Cl_3(AsMe_3)_6]^{2+}$	11 600	2.16	1.90
$[Ru_2Br_3(AsMe_3)_6]^{2+}$	10 800	2.22	1.85
$[Ru_2Cl_3(AsMe_2Ph)_6]^{2+}$	10 510	2.18	1.87
$[Ru_2Br_3(AsMe_2Ph)_6]^{2+}$	10 100	2.24	1.77
$[Ru_2Cl_3(PMe_3)_6]^{2+}$	9 350	2.23	1.82
$[Ru_2Br_3(PMe_3)_6]^{2+}$	8 800	2.28	1.65
$[Ru_2Cl_3(AsMe_3)_4(PPh_3)_2]^{2+}$	8 700	2.26	1.73
$[Ru_2Cl_3(PMe_2Ph)_6]^{2+}$	7 950	2.29	1.68
$[Ru_2Cl_3(PEt_3)_6]^{2+}$	7 460	2.32	1.65
$[Ru_2Br_3(PMe_2Ph)_6]^{2+}$	7 400	2.34	*f*
$[Ru_2Cl_3(PEtPh_2)_6]^{2+}$	6 980	2.32	1.50
$[Ru_2Br_3(PEt_3)_6]^{2+}$	6 500	2.35	*f*
$[Ru_2Cl_3(PEt_2Ph)_6]^{2+}$	6 250	2.32	1.40
$[Ru_2Cl_3(PMePh_2)_6]^{2+}$	4 950	2.35	*f*
$[Ru_2Br_3(PEt_2Ph)_6]^{2+}$	4 800	2.35	*f*

[a] Recorded in CH_2Cl_2 at 213 K unless stated otherwise. [b] Recorded in frozen-glass CH_2Cl_2 solutions containing $[NBu^n_4][BF_4]$ (0.5 mol dm^{-3}) at 20 K, unless stated otherwise. [c] Visible spectrum recorded in dmso,[10] EPR in dmso–glycerol glass at 60 K.[11] [d] The EPR spectrum was recorded as dmso glass at 10 K.[14] [e] Visible spectrum recorded in aqueous solution, EPR as aqueous glass at 150 K. [f] $g_\parallel$ too broad and weak to assign.

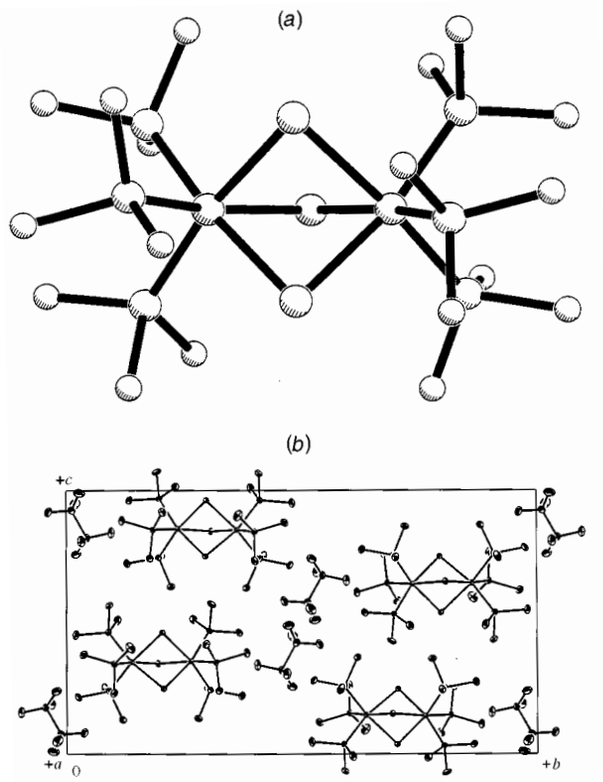

Fig. 9 X-Ray structural data for $[Ru_2(\mu\text{-}Cl)_3(AsMe_3)_6][CF_3SO_3]$: (*a*) view of the binuclear cation, (*b*) projection of the monoclinic unit-cell. Crystal data: space group $P2_1/n$ (no. 14), $a = 9.767(2)$, $b = 26.699(2)$, $c = 15.449(1)$ Å, $\beta = 91.53(1)°$, $Z = 4$, $D_c = 1.942$ g cm^{-3}, Cu-Kα radiation, 6143 unique reflections ($R_{int} = 0.037$). This compound is strictly isomorphous with its PMe_3 and μ-Br analogues (see text)

the present electrogenerated hexakis-arsine and -phosphine dimers. These delocalised, binuclear $S = \frac{1}{2}$ paramagnets display an axially symmetric g tensor. That is, $g_\parallel = g_z$ and $g_\perp = g_x$, g_y where z coincides with the Ru–Ru axis and so with the principal alignment of the singly occupied σ* orbital, as expected in such delocalised confacial systems.[38] Of necessity, $g_\perp > 2$ and $g_\parallel < 2$, and the numerically greater component is associated with the more intense signal. In the limit where the axial perturbation provided by metal–metal bonding greatly exceeds local spin–orbit coupling, exemplified here by 'blues' such as $[Ru_2Cl_3(NH_3)_6]^{2+}$, $g_\perp$ and $g_\parallel$ should both approach 2.0.[11,39] The EPR data are collated in Table 5, where the compounds are arranged in descending order according to their characteristic $\sigma \longrightarrow \sigma^*$ band energy. There is a well known technical difficulty in tracking the $g_\parallel$ resonance as it diminishes in value, because the signal becomes progressively weaker and broader and eventually undetectable when $g_\parallel <$ *ca.* 1.4. By inspection, the present tertiary arsine and phosphine complexes form a continuous series with progressively diverging $g_\perp$ and $g_\parallel$ values. The mixed-ligand complex falls smoothly into the sequence with no evidence of its lower formal symmetry. Descending Table 5, $g_\perp$ increases smoothly to ≈2.35 for $[Ru_2Br_3(PEt_3)_6]^{2+}$ and then levels off, whereas $g_\parallel$ decreases slowly at first and then increasingly steeply from its initial value of 1.90. This two-branch trend in $g_\perp$ and $g_\parallel$ (presented here as a function of W_σ) adheres closely to the classical g-tensor behaviour for increasingly trigonally distorted $S = \frac{1}{2}$ systems.

The detailed ligand-field analysis for this body of compounds, and the fundamental quantitative correlation of the axial g tensor with the associated metal–metal σ bonding, will be developed elsewhere.[40] Here we only wish to stress our qualitative conclusions. The smooth progression in EPR parameters independently confirms the overall ranking of compounds within the family. Despite the marked contrast between the first and last entry in Table 5 there is no evidence of a dichotomy in electronic ground state. (A distinctly different g tensor should arise in the so-far hypothetical situation of a frankly trapped $[Ru^{2+}Ru^{3+}]$ ground state.[39]) Accordingly, an orderly empirical trend is evident whether the strength of electronic coupling is measured by voltammetry (ΔE^1_2), near-IR spectroscopy ($\nu_{\sigma\longrightarrow\sigma^*}$), or electron paramagnetic resonances ($g_\perp$ and $g_\parallel$). It is worth noting that if the cross-over assignment mentioned earlier were adopted, with $\nu_{\sigma\longrightarrow\sigma^*}$ somehow falling lower than $\nu_{\delta_z^*\longrightarrow\sigma^*}$ for the majority of phosphine complexes, then the optical aspect of this correlation would break down.

In summary, comparative EPR data play a significant part in helping to place the 11-e AsR_3 and PR_3 confacial complexes in context with their blue ammine analogues. The metal–metal interaction, independently measured by $\nu_{\sigma\longrightarrow\sigma^*}$, turns out to dominate the trigonal-field distortion and this is reflected in the behaviour of the g tensor. For this reason the EPR spectra are particularly deserving of rigorous analysis, and this will be the subject of a further report.[40]

Structural data

***(i)* II,II compounds.** We recently reported the first crystallographic data for hexakisarsinediruthenium complexes,[41] specifically for $[Ru_2Cl_3(AsMe_2Ph)_6]^+$ and $[Ru_2Br_3(AsMe_3)_6]^+$ in the form of their triflate salts. The X-ray structural examination has now been extended from $[Ru_2Br_3(AsMe_3)_6]^+$ to the corresponding $[Ru_2Cl_3(AsMe_3)_6]^+$, $[Ru_2Br_3(PMe_3)_6]^+$ and $[Ru_2Cl_3(PMe_3)_6]^+$ triflates, so completing a strict isostructural series.[1,42] Fig. 9 illustrates the relatively uncluttered molecular structure and simple arrangement within the unit cell, common to all four. The most pertinent dimensions are collected in Table 6, where the $AsMe_3$ and $AsMe_2Ph$ compounds are compared with their exact congeners and also with a wider range of phosphine analogues. Perhaps surprisingly, it appears that no crystal structure has been reported previously for any $[Ru_2Br_3(PR_3)_6]^+$ complex.

The structural data in Table 6 refer to the 12-e $Ru_2^{II,II}$ oxidation state which of course has no net metal–metal bonding.

Table 6 Structural parameters for triply halide-bridged diruthenium complexes

Complex	Ru–Ru/Å	Ru–X[a]/Å	Ru–L[a]/Å	Ru–X–Ru[a]/°	L–Ru–L[a]/°	Ref.[b]
$[Ru_2Cl_3(AsMe_3)_6]^+$	3.263(1)	2.48	2.37	82.4	95.0	t.w.
$[Ru_2Cl_3(AsMe_2Ph)_6]^+$	3.275(1)	2.46	2.40	83.5	95.4	t.w., 41
$[Ru_2Cl_3(PMe_3)_6]^+$	3.374(6)	2.50	2.26	85.1	95.2	t.w., 41
$[Ru_2Cl_3(PMe_3)_6]^{+c}$	(3.27_5)	(2.48)	(2.25)	(82.9)	(95.4)	43
$[Ru_2Cl_3(PMe_2Ph)_6]^+$	3.394(3)	2.49	2.29	86.0	96	22
$[Ru_2Cl_3(PEt_2Ph)_6]^+$	3.44	2.48	2.32	87.9	96.9	24
$[Ru_2Cl_3(PBu_3)_6]^+$	3.39	2.49	2.30	86.2	96.6	37
$[Ru_2Cl_3\{MeC(CH_2PPh_2)_3\}_2]^+$	3.455	2.49	2.31	87.8	88.3	25
$[Ru_2Br_3(AsMe_3)_6]^+$	3.413(1)	2.61	2.38	81.8	94.6	t.w., 41
$[Ru_2Br_3(PMe_3)_6]^+$	3.5365(8)	2.64	2.27	84.2	95.0	t.w.

[a] Averaged values. [b] t.w. = This work: $CF_3SO_3^-$ salt. [c] Less appropriate comparison; this structure has highly disordered BF_4^- counter ions with an uncertain spatial relationship to the cation. No special cation–anion contacts are apparent in the unit-cell of the present family of $CF_3SO_3^-$ salts.

The wide separation of the halide-bridged metal centres, ranging from 3.26 to 3.46 Å, is in accord with this, and presumably reflects the mutual electrostatic repulsion of the two divalent ions. However, the $Ru_2^{II,II}$ arsine complexes have a distinctly smaller Ru–X–Ru bridgehead angle than their phosphine counterparts, by 2.5° or more, with an associated contraction of at least 0.1 Å in the non-bonded Ru···Ru separation.

It is very instructive that the systematic structural distinction between the binuclear arsine and phosphine complexes is encountered at the closed-shell II,II level, because this requires an explanation which makes no appeal to metal–metal bonding. The source of the discriminatory effect on the geometry of the $\{Ru(\mu\text{-}X)_3Ru\}^+$ core is not immediately obvious, since the μ-Cl/$AsMe_3$ complex and its μ-Cl/PMe_3 analogue have indistinguishable exterior cone angles in the RuL_3 face (95.0 *vs.* 95.2°) and comparable *trans* influences on the bridging Ru–Cl bond length (2.48 *vs.* 2.50 Å). Similar geometric conclusions apply to every pair of exact As/P congeners presented in Table 6.‡ Among the phosphine derivatives themselves, the PMe_3 and PMe_2Ph complexes have the shortest Ru···Ru distance and the most acute bridgehead angle; these are the same compounds which, upon oxidation, yield near-infrared spectra most nearly resembling the classical 'blues' and their AsR_3 analogues (Fig. 7).

Despite the similarity in cone angles mentioned above, the structural distinction between the AsR_3 and PR_3 binuclear complexes appears to be a rather subtle consequence of the Ru–As bond being longer by ≈0.12 Å. This outward displacement of the As atoms alleviates the repulsive C–H/X contacts between the ligand substituents and the bridging $\{X_3\}$ array,[41] which in the PR_3-capped analogues fall some 0.25 Å below the sum of the van der Waals radii. Related C–H/μ-X contacts are already familiar in tmtacn- and tacn-capped blues.[14,15] In summary, the new structural data gathered for the closed-shell systems reveal an unexpected but distinctive capacity for the arsine ligands so far studied ($AsMe_3$ and $AsMe_2Ph$) to favour closer Ru···Ru contact, compared to their exact phosphine congeners. These discriminatory effects are expected to carry over to the corresponding II,III states (see below), and so to influence their electronic behaviour.

***(ii)* II,III compounds.** In the case of the oxidised (11-e) systems, $[L_3Ru(\mu\text{-}X)_3RuL_3]^{2+}$, no crystal structures are available for L = AsR_3 or PR_3. However, it is important to have some guidance on the geometry of the oxidised forms, since their electronic properties are the main focus of the present paper. Recent SCF-Xα computations in our laboratory[4,44] have established a faithful quantitative match between the observed and calculated $\nu_{\sigma\longrightarrow\sigma^*}$ energies for seven ruthenium ammine and triazanonane 'blues'§ of known structure. An orderly near-linear relationship emerges between the calculated $\nu_{\sigma\longrightarrow\sigma^*}$ energy and the parameter *r*(Ru–Ru), when the latter is made to vary between 2.6 and 3.1 Å. Extension of this methodology leads to six separate correlation curves (constructed for L = NH_3, AsH_3 or PH_3; X = Cl or Br)[44] which link the observed $\nu_{\sigma\longrightarrow\sigma^*}$ energies with the implied equilibrium separation, *r*(Ru–Ru), in each case. For example, whereas *r*(Ru–Ru) is known crystallographically[45] to be 2.76 Å for the μ-Cl/NH_3 system, it is estimated to expand to 2.92 Å for μ-Cl/$AsMe_3$ and to 3.00 Å for μ-Cl/PMe_3. For the corresponding bromides, on the evidence of the $\nu_{\sigma\longrightarrow\sigma^*}$ band energies, *r*(Ru–Ru) expands from the known 2.85 Å in the μ-Br/NH_3 system[46] to 3.00 Å for μ-Br/$AsMe_3$ and 3.09 Å for μ-Br/PMe_3.

Considerable experimental support for these metrical predictions is provided by the closely related neutral mixed-valence complex $[(Me_3P)_2ClRu(\mu\text{-}Cl)_3RuCl(PMe_3)_2]$, with eclipsed PMe_3 ligands, which has a crystallographically determined[37] Ru–Ru separation of 2.992(1) Å. This should, if anything, be slightly shorter than in the hexa-PMe_3 11-e analogue, estimated above at 3.00 Å, because of the anticipated enhancement of metal–metal bonding by the two terminal chloride ligands. Recently, Gamelin *et al.*[47] have independently applied SCF-Xα methodology with marked success to probing molecular distortion in the σσ* excited state of isoelectronic $[(tmtacn)Fe(\mu\text{-}OH)_3Fe(tmtacn)]^{2+}$. In this closely related approach, the Xα-derived transition energy, $\nu_{\sigma\longrightarrow\sigma^*}$, was likewise calculated for varied *r*(Fe–Fe) separations, corresponding to favoured normal coordinate (a_1') distortions from the equilibrium geometry.¶

In summary, these computational advances have enabled estimation of the hemi-bonded Ru–Ru separation from the observed near-IR σ ⟶ σ* transition energy within each $[L_3Ru(\mu\text{-}X)_3RuL_3]^{2+}$ family. Progressive lengthening in the sequence L = NR_3, AsR_3, PR_3 is predicted, with increments of 0.15 and then 0.1 Å, respectively. It should be emphasised that according to our analysis the contrasting behaviour of the PR_3 and AsR_3 systems is an electronic consequence of structural differences (selective crowding), rather than a structural consequence of electronic differences between P and As donor atoms.

‡ An earlier X-ray analysis[43] of $[Ru_2Cl_3(PMe_3)_6]BF_4$ suggested a still smaller Ru···Ru distance and bridge angle for this complex, but this is probably misleading (*cf.* Table 6), and certainly a less reliable basis for comparison than the data now assembled for the crystallographically isomorphous triflates.

§ New structural and optical data for several ammine blues kindly provided by Clucas and co-workers[15] were crucial in the calibration of these calculations.

¶ This more detailed study[47] embraced analysis of the resonance-Raman excitation profile and optical band shape for the $Fe_2^{II,III}$ σ ⟶ σ* band near 13 500 cm^{-1}.

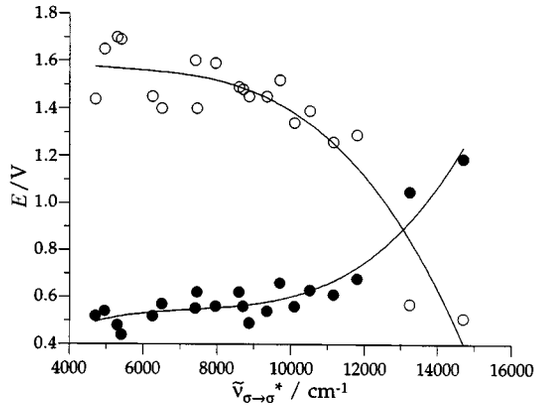

Fig. 10 Correlations of $\nu_{\sigma\longrightarrow\sigma^*}$ for $[Ru_2(\mu\text{-}X)_3L_6]^{2+}$ with E_{av} (open circles) and $\Delta E_{\frac{1}{2}}$ (closed circles). The curves are mathematically generated polynomials of best fit. Data for μ-Cl and μ-Br complexes in Table 3 have been merged, exaggerating the true scatter (*cf.* Fig. 4)

Overall trends in structure, bonding and spectroscopy

The wide-ranging behaviour surveyed above can now be understood to reflect a remarkable three-fold variation overall in the metal–metal σ-bonding interaction within the family of confacial $[L_3Ru(\mu\text{-}X)_3RuL_3]^{2+}$ complexes. The resonance energy (W_σ), as identified with half the $\sigma\longrightarrow\sigma^*$ promotion energy (Table 5), is found to increase from ≈2500 cm^{-1} for $[Ru_2Cl_3(PMePh_2)_6]^{2+}$ to ≈6000 cm^{-1} for $[Ru_2Cl_3(AsMe_3)_6]^{2+}$, with a parallel change in the μ-Br series. This trend smoothly connects with isostructural ammine systems where W_σ rises to ≈8000 cm^{-1} for $[Ru_2Cl_3(NH_3)_6]^{2+}$. As noted above, the three-fold variation in W_σ is fully consistent with the non-linear but coherent progression in the experimentally determined axial *g* tensor, and of course with the estimated change in *r*(Ru–Ru).

This sequence in the $\nu_{\sigma\longrightarrow\sigma^*}$ energies is all the more striking because it is non-periodic ($NR_3 > AsR_3 > PR_3$), for reasons canvassed above. In this respect, it matches the relative ease of oxidation of the binuclear systems as measured empirically by E_{av}. There is also a scattered but unmistakable correlation of the $\sigma\longrightarrow\sigma^*$ band with the gap in oxidation potentials, $\Delta E_{\frac{1}{2}}$ which is further examined below. These two progressions are compared in Fig. 10. Their complementary nature follows naturally from the underlying relationship between E_{av} and $\Delta E_{\frac{1}{2}}$ presented in Fig. 4.

Trends in comproportionation energy, ΔG_c ($=nF\Delta E_{\frac{1}{2}}$)

It is often said that increased metal–metal interaction in redox-active binuclear complexes should be accompanied by increasing separation of the successive couples ($\Delta E_{\frac{1}{2}}$). This axiom was originally developed[48] in the context of weakly coupled (Class II[49]) mixed-valence systems in which the contribution of the potential two-electron bond in the associated 10-e state could be explicitly discounted. In contrast, for fully delocalised (Class III[49]) systems the proposition seems to us neither self-evident nor inevitable, despite being nicely exemplified by the present $[L_3Ru(\mu\text{-}X)_3RuL_3]^{z+}$ family (Fig. 10). The physical significance of the $\Delta E_{\frac{1}{2}}$ parameter, which ranges widely from 0.45 to 1.2 V for the present compounds, is therefore examined below.

Certainly, $\Delta E_{\frac{1}{2}}$ is thermodynamically equivalent to ΔG_c, the free energy of comproportionation of $M_2^{III,III} + M_2^{II,II}$ to form 2 mol of $M_2^{II,III}$, *i.e.* $\Delta G_c = -nF\Delta E_{\frac{1}{2}}$. So the question becomes: 'within a family of electronically and structurally related binuclear compounds, under what circumstances will the comproportionation energy systematically reflect variations in the M–M bond strength of the mixed-valence state?'

For three-electron hemi-bonded systems in general, comproportionation is bound to be strongly exothermic, since $[\{\sigma^2\sigma^{*1}\} + \{\sigma^2\sigma^{*1}\}]$ is greatly favoured over $[\{\sigma^2\sigma^{*0}\} + \{\sigma^2\sigma^{*2}\}]$ in the distribution of six frontier electrons between two molecules, with less net electron–electron repulsion and a more symmetric charge distribution overall. However, this universal effect will not necessarily engender differences in $\Delta E_{\frac{1}{2}}$ in a series of similar binuclear compounds. Three possibilities can be considered, according to the effect of oxidation state on W_σ.

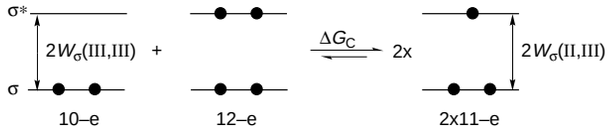

Scheme 3

On the simplest assumption of *constant splitting* between σ and σ* orbitals across the three successive oxidation states as shown in Scheme 3 (though the notional splitting at the non-bonded 12-e level is immaterial), the gap in successive oxidation potentials clearly owes nothing to the W_σ contributions, which cancel out, and $\Delta E_{\frac{1}{2}}$ depends rather on the nett repulsion experienced by electrons occupying the redox-active σ* orbital. This term might be expected not to vary significantly within the series of isostructural $[Ru(\mu\text{-}X)_3Ru]^{z+}$ dimers, unless the correlation energy associated with various $\sigma^2\sigma^{*n}$ configurations (Scheme 3; $n = 0, 1, 2$) changes systematically as the quality of the σ bond increases. We would welcome comment on this question, both in general terms and in relation to the data in Fig. 10.

If, instead, we suppose the σ–σ* splitting *diminishes* upon oxidation to the 10-e state, then the connection between enhanced metal–metal bonding in the mixed-valence state and increased $\Delta E_{\frac{1}{2}}$ becomes straightforward. Comproportionation is made more exothermic to the extent that W_σ(III,III) < W_σ(II,III), because $1 \times \{\sigma^2\sigma^{*0}\}_{III,III}$ then carries less bond-energy overall than does $2 \times \{\sigma^2\sigma^{*1}\}_{II,III}$. It is reasonable (though not inevitable) that the sequence from non-bonded $\sigma^2\sigma^{*2}$ through hemi-bonded $\sigma^2\sigma^{*1}$ to the $\sigma^2\sigma^{*0}$ configuration can culminate in a weakened two-electron bond, because progressive oxidation of the binuclear core is accompanied by radial contraction of the single-ion d orbitals and by increased electrostatic repulsion between the two positive metal centres. These are strong effects which may outweigh the increasing bond order.[4,50]

On the other hand, it is equally possible that in other cases the two-electron single bond 'wins out' over these effects, with synergistic establishment of a shorter M–M separation and thereby a *greater* σ–σ* splitting at the 10-e level, notwithstanding the higher overall oxidation state. This would lead to inversion of the conventional Δ*E*/binuclear-interaction relationship, with $\Delta E_{\frac{1}{2}}$ made smaller by the favourable W_σ(III,III) term.

To evaluate these three alternatives for a real chemical system one needs to assemble reliable information on the electronic σ–σ* splitting (= $2W_\sigma$) and the associated M–M distance in both 11- and 10-e states, a potentially difficult task. In the context of triply halide-bridged diruthenium complexes, the factual and circumstantial evidence is most complete for the $[Ru_2X_9]^{z-}$ systems (X = Cl or Br), which are positioned neatly between the ammine 'blues' and the analogous arsines according to their optical and voltammetric behaviour. The metal–metal distance is believed to contract by ≈0.15 Å between the $Ru_2^{II,III}$ and $Ru_2^{III,III}$ nonahalides. Overall, the estimated σ–σ* splitting is almost unaltered upon oxidation to the III,III state (decreasing from 10 100 cm^{-1} for $[Ru_2Br_9]^{4-}$ to 9 400 cm^{-1} for $[Ru_2Br_9]^{3-}$, stationary at 12 300 cm^{-1} for $[Ru_2Cl_9]^{4-}$ and $[Ru_2Cl_9]^{3-}$).[8,44] These systems provide a clear example of metal–metal bonding persisting in the 10-e state. They approach the simple premise of a constant W_σ, presumably through the interplay of the formal doubling of bond order with the countervailing influence of orbital contraction and increased cation–cation (M^{z+}/M^{z+}) repulsion.

In summary, the observed increase in the electrode potential

separation ($\Delta E_{\frac{1}{2}}$) within a given family of binuclear compounds may well be attributable in the conventional way to a parallel trend in the M–M bond strength at the mixed-valence level, but only if the W_σ term falls significantly and proportionately for each system upon further oxidation. The evidence is incomplete for the present AsR_3- and PR_3-capped compounds as yet, because of the reactive nature of the 10-e state. However, we believe that a pronounced decrease in W_σ between the II,III and III,III levels plays a major role in the behaviour of sterically hindered $[Ru_2X_3(AsR_3)_6]^{2+}$ and $[Ru_2X_3(PR_3)_6]^{2+}$ systems.

Conclusion

The discovery of mixed-valence $[(R_3As)_3Ru(\mu\text{-}X)_3Ru(AsR_3)_3]^{2+}$ complexes has placed the long-standing phosphine-capped analogues in a proper context and clarified their non-classical near-IR spectra. Unlike the new AsR_3-capped ruthenium 'blues', there is also considerable circumstantial evidence that the hexakisphosphine complexes, while still delocalised, are close to the point where the driving force for forming the one-electron bond is marginal. This evidence includes the orderly voltammetric data which places 11-e $[(R_3P)_3Ru(\mu\text{-}X)_3Ru(PR_3)_3]^{2+}$ and $[(R_3P)_2XRu(\mu\text{-}X)_3RuX(PR_3)_2]$ firmly within the general family of confacial compounds of stoichiometry $[(R_3P)_{3-x}X_xRu(\mu\text{-}X)_3RuX_y(PR_3)_{3-y}]^{2-x-y}$, even though the latter[7,16,30,36,37] are localised when $x \neq y$.

The behaviour of newly established heterobimetallic complexes[1,2,40] of the form $[(R_3P)_3Ru(\mu\text{-}X_3)Os(PR_3)_3]^+$ is even more suggestive. In each {Ru,Os} complex the first (osmium-centred) oxidation coincides exactly with E_1 of the $\{Os_2\}$ analogue while the more difficult (ruthenium-centred) oxidation coincides exactly with E_2 of the $\{Ru_2\}$ analogue. The mixed-metal complexes are necessarily localised (= $Ru^{II}Os^{III}$) in the 11-e state, so the simple transferable nature of the electrode potentials confirms the marginal influence (evidently <20 mV) of the prospective hemi-bond in the parent $\{Ru_2\}$ and $\{Os_2\}$ systems.

The confacial $Os_2^{II,III}$ phosphine-capped complexes show almost complete transfer of intensity to the lower-frequency band,[2,18] which has the effect of reversing the appearance of the visible/near-infrared absorption spectrum relative to classical blues. Contrary to general expectation, they are probably better candidates for valency trapping than their $Ru_2^{II,III}$ analogues! The much greater single-ion spin–orbit coupling of Os^{3+} provides a driving force to resist delocalisation and to transform the $\{Os_2\}$ species from Class III to Class II systems. The absence of an effective three-electron hemi-bond would explain the similarity of the metal–metal separation in the crystal structures[18] of $[(Et_3P)_3Os(\mu\text{-}Cl)_3Os(PEt_3)_3]^+$ and $[(Et_3P)_3Os(\mu\text{-}Cl)_3Os(PEt_3)_3]^{2+}$ where Os···Os 3.473(1) and 3.406(1) Å respectively. It would also explain the unexpected contraction in $\Delta E_{\frac{1}{2}}$ for the $\{Os_2\}$ systems noted earlier, in the electrochemistry discussion.

Meticulous studies by Yellowlees and co-workers[18] established that the relatively intense, structured near-infrared absorption of the 11-e diosmium compounds (near 5000 cm^{-1}) is unshifted by wide variation in the dipolar nature of the solvent, which is normally indicative of electronic promotion within a fully delocalised manifold.[51] However, this invariance would be equally well explained if the near-IR spectrum is dominated by single-ion interconfigurational bands characteristic of the localised osmium(III) centre.‖

This proposition (that $Ru_2^{II,III}$ systems are delocalised whereas their osmium analogues may be trapped) underscores the electronic subtlety of this general class of confacial dimers. Given the enforced proximity of the two halide-bridged metal ions, the limiting physical properties of such notionally trapped confacial systems are of keen interest. Inevitably, there will be a domain which is transitional between the two clear-cut descriptions. Yeomans[1] foresaw it would be possible to generate genuine diosmium 'blues' having classical near-IR spectra by replacing PR_3 with NR_3 (or possibly with AsR_3), though these preparative targets have been elusive to date. The first report of tervalent $[(tmtacn)Os(\mu\text{-}Cl_3)Os(tmtacn)]^{3+}$ and its tacn counterpart (Os–Os 2.667 Å) has now appeared; these important complexes are readily reduced to red-purple solutions of the presumed dication, and have $\Delta E_{\frac{1}{2}} = 1.0$ V.[52] The new $Os_2^{III,III}$ ammine systems clearly resemble isovalent $[Os_2Br_9]^{3-}$ which has a comparable Os–Os single bond (2.880 Å),[53,54] especially if allowance is made for replacing μ-Cl by μ-Br. The corresponding 11-e complexes $[Os_2Cl_9]^{4-}$ and $[Os_2Br_9]^{4-}$ have so far proved too short-lived for their near-IR spectra to be collected, even at −215 K.[53]

At the other extreme, it might be possible to induce electronic trapping in co-ordinatively symmetric $[L_3Ru(\mu\text{-}X)_3RuL_3]^{2+}$ systems if a pattern of terminal ligation is found where W_σ diminishes by a further 500 to 1000 cm^{-1}. The newly revealed discriminatory effects of steric compression between the capping and bridging ligands could be useful in this. The $Ru_2^{II,III}$ oxidation level becomes harder to reach as coupling diminishes, but our projections (Fig. 10) suggest the trapped-valence state can be approached without an impossibly high electrogeneration potential.

This study has resolved long-standing difficulties by addressing a range of information on an instructive family of compounds established through strategic synthesis. The 11-e confacial bioctahedral system provides an ideal framework for systematic modulation of mixed valency, and we trust the present contribution will stimulate further interest and new investigations. In closing, we would like to pay tribute to the influence of the late Professor Joseph Chatt, FRS, and Dr. T. A. (Tony) Stephenson, who made pioneering contributions in this area.**

Experimental

General

The following compounds were prepared by standard methods: $[RuCl_2(PPh_3)_3]$ and $[RuBr_2(PPh_3)_3]$,[56] $K_3[Ru_2Cl_9]$ and $K_3[Ru_2Br_9]$,[30,31] $AsMePh_2$,[57] $PMePh_2$ and PMe_3.[58] Other phosphine and arsine ligands were from Aldrich Chemical Co., and 1,1,1-tris(diphenylphosphinomethyl)ethane from Strem Chemicals Inc. Triflic acid (CF_3SO_3H) was vacuum-distilled prior to use. All reactions were carried out using purified deoxygenated solvents under N_2, but the solid products listed below were handled in air. The CH_2Cl_2 for electrochemical, spectroelectrochemical and EPR measurements was freshly distilled from CaH_2 before use. Elemental analyses were performed by the Research School of Chemistry Microanalysis Unit. The NMR spectra were recorded using a Varian Gemini 300BB spectrometer, with shifts referred to internal $SiMe_4$ (^1H) and external 85% H_3PO_4 in D_2O (^{31}P-{^1H}).

All electrochemical measurements were performed on chilled solutions using a PAR 170 electrochemistry system; typical scan rates were 100 mV s^{-1} for cyclic voltammetry and 10 mV s^{-1} for alternating current voltammetry. The latter were recorded with positive feedback resistance compensation and phase-sensitive detection ($\omega = 205$ Hz). Electrolyte solutions contained 0.5 mol dm^{-3} $[NBu^n_4][BF_4]$ and *ca.* 10^{-3} mol dm^{-3} of the complex in CH_2Cl_2. The solutions were purged and main-

‖ The invariance of visible/near-IR spectra of frankly localised $[(R_3P)_3Ru(\mu\text{-}X_3)Os(PR_3)_3]^{2+}$ in the same range of solvents (refs. 1 and 40) reinforces this argument, and shows that the absence of solvatochromism need not indicate delocalisation in complexes of this form.

** *Note added at proof*: Levason and co-workers[55] have reported crystal structures for three new 11-e $[L_2XRu(\mu\text{-}X)_3RuXL_2]$ complexes, where L/X = PMe_2Ph/Br, $AsMe_2Ph$/Br or $AsMe_2Ph$/I, having r(Ru–Ru) = 3.083(2), 2.941(2) or 3.197(5) Å, respectively. Our projections for $[Ru_2X_3L_6]^{2+}$ fit well with these instructive data.

tained under an atmosphere of N_2. The jacketed 10 cm^3 glass cell was fitted with a platinum-disc working electrode (0.5 mm diameter), platinum auxiliary electrode, Ag–AgCl reference electrode (against which ferrocene is oxidised at +0.55 V) isolated by a fritted salt bridge, and a submerged digital thermometer probe. An electronically controlled Lauda RL6 cryostat bath, circulating dry chilled MeOH, was used to maintain the low temperature.

Electronic spectra (45 000–3125 cm^{-1}) were recorded with a Perkin-Elmer Lambda 9 spectrophotometer. Spectra of oxidised species were obtained at 213 K by electrogeneration within a cryostatted optical semi-thin-layer electrochemical cell (path length 0.5 mm), described previously,[59] mounted within the sample compartment of the spectrophotometer. Solutions contained 0.5 mol dm^{-3} $[NBu^n_4][BF_4]$ in CH_2Cl_2. The electrogeneration potential was set *ca.* 200 mV beyond $E_{\frac{1}{2}}$ for each complex.

Solutions of mixed-valence complexes for EPR studies were generated by exhaustive electrolysis at 213 K in an all-glass jacketed H-pattern cell, constructed in our laboratory, with two frits separating the anode and cathode compartments. The anolyte solutions (working volume *ca.* 5 cm^3) contained *ca.* 10^{-2} mol dm^{-3} $[Ru_2(\mu\text{-}X)_3L_6]^+$ and 0.5 mol dm^{-3} $[NBu^n_4][BF_4]$ in CH_2Cl_2. Each bulk oxidation was performed at a cylindrical platinum-gauze electrode and monitored at intervals by stirred d.c. (and a.c.) voltammetry at an independent working electrode. The EPR spectra of the glassy frozen electrolyte solutions at 20 K were recorded using a Varian X-band spectrometer fitted with an Oxford Instruments helium cryostat.

Synthetic procedures

(1) Tri-μ-chloro-bis[tris(trimethylarsine)ruthenium(II)] triflate. A mixture of $K_3[Ru_2Cl_9]$ (0.15 g, 0.23 mmol) and $AsMe_3$ (0.25 g, 2.1 mmol) in ethanol (45 cm^3) and distilled water (15 cm^3) was heated at reflux for 24 h. The solvent was evaporated *in vacuo* to leave a yellow residue which was washed with Et_2O, dissolved in CH_2Cl_2, filtered and heated at reflux with 0.1 mol dm^{-3} CF_3SO_3H in methanol (3 cm^3, 0.3 mmol) for 16 h. The solvent was evaporated *in vacuo* and the residue recrystallised from CH_2Cl_2–Et_2O. Yield of $[Ru_2(\mu\text{-}Cl)_3(AsMe_3)_6][CF_3SO_3]$ 0.060 g (22%) (Found: C, 19.0; H, 4.9; Cl, 9.4. $C_{19}H_{54}As_6Cl_3F_3O_3Ru_2S$ requires C, 19.4; H, 4.6; Cl, 9.0%). ^1H NMR (CD_2Cl_2): δ 1.35 (s, CH_3).

(2) Tri-μ-bromo-bis[tris(trimethylarsine)ruthenium(II)] triflate. Prepared as in (1), heating $K_3[Ru_2Br_9]$ (0.20 g, 0.19 mmol) and $AsMe_3$ (0.15 g, 1.25 mmol) in ethanol (40 cm^3) and water (10 cm^3) for 40 h. Yield of $[Ru_2(\mu\text{-}Br)_3(AsMe_3)_6][CF_3SO_3]$ 0.041 g (16%) (Found: C, 17.5; H, 4.3; Br, 18.4. $C_{19}H_{54}As_6Br_3F_3O_3Ru_2S$ requires C, 17.4; H, 4.15; Br, 18.3%). ^1H NMR (CD_2Cl_2): δ 1.41 (s, CH_3).

(3) Tri-μ-chloro-bis[tris(dimethylphenylarsine)ruthenium(II)] triflate. Prepared as in (1) by heating $K_3[Ru_2Cl_9]$ (0.15 g, 0.23 mmol) and $AsMe_2Ph$ (0.25 g, 1.4 mmol) in ethanol (40 cm^3) and water (10 cm^3) for 16 h. Yield of $[Ru_2(\mu\text{-}Cl)_3(AsMe_2Ph)_6][CF_3SO_3]$ 0.15 g (42%) (Found: C, 37.8; H, 4.5; Cl, 6.8. $C_{49}H_{66}As_6Cl_3F_3O_3Ru_2S$ requires C, 38.0; H, 4.3; Cl, 6.9%). ^1H NMR (CD_2Cl_2): δ 1.45 (6 H, s, CH_3) and 7.15–7.40 (5 H, m, C_6H_5).

(4) Tri-μ-bromo-bis[tris(dimethylphenylarsine)ruthenium(II)] triflate. Prepared as in (1) by heating $K_3[Ru_2Br_9]$ (0.15 g, 0.14 mmol) and $AsMe_2Ph$ (0.25 g, 1.4 mmol) in ethanol (40 cm^3) and water (10 cm^3) for 16 h. Yield of $[Ru_2(\mu\text{-}Br)_3(AsMe_2Ph)_6][CF_3SO_3]$ 0.032 g (13%) (Found: C, 34.5; H, 4.0; Br, 14.1. $C_{49}H_{66}As_6Br_3F_3O_3Ru_2S$ requires C, 35.0; H, 3.95; Br, 14.2%). ^1H NMR (CD_2Cl_2): δ 1.52 (6 H, s, CH_3) and 7.12–7.41 (5 H, m, C_6H_5).

(5) Tri-μ-chloro-bis[tris(methyldiphenylarsine)ruthenium(II)] triflate. Prepared as in (1) by heating $K_3[Ru_2Cl_9]$ (0.15 g, 0.23 mmol) and $AsMePh_2$ (0.35 g, 1.4 mmol) in ethanol (40 cm^3) and water (10 cm^3) for 15 h. Yield of $[Ru_2(\mu\text{-}Cl)_3(AsMePh_2)_6][CF_3SO_3]$ 0.14 g (32%) (Found: C, 49.0; H, 4.2; Cl, 5.6. $C_{79}H_{78}As_6Cl_3F_3O_3Ru_2S$ requires C, 49.35; H, 4.1; Cl, 5.5%). ^1H NMR (CD_2Cl_2): δ 1.60 (3 H, s, CH_3) and 7.00–7.34 (10 H, m, C_6H_5).

(6) Tri-μ-bromo-bis[tris(methyldiphenylarsine)ruthenium(II)] triflate. Prepared as in (1) by heating $K_3[Ru_2Br_9]$ (0.20 g, 0.19 mmol) and $AsMePh_2$ (0.35 g, 1.4 mmol) in ethanol (45 cm^3) and water (15 cm^3) for 16 h. Yield of $[Ru_2(\mu\text{-}Br)_3(AsMePh_2)_6][CF_3SO_3]$ 0.012 g (3%, similar in four independent preparations) (Found: C, 44.9; H, 4.0; Br, 13.1. $C_{79}H_{78}As_6Br_3F_3O_3Ru_2S$ requires C, 46.15; H, 3.8; Br, 11.7%). ^1H NMR (CD_2Cl_2): δ 1.70 (3 H, s, CH_3) and 6.95–7.30 (10 H, m, C_6H_5). FAB mass spectrum: m/z = 1906.9 (1906.9). Microanalytical data did not improve despite several recrystallisations and plentiful instrumental evidence of correct constitution and apparent purity.

(7) Tri-μ-chloro-bis[bis(trimethylarsine)(triphenylphosphine)ruthenium(II)] triflate. To a suspension of $[RuCl_2(PPh_3)_3]$ (0.50 g, 0.26 mmol) in ethanol (60 cm^3) was added $AsMe_3$ (0.40 g, 3.3 mmol). The mixture was heated at reflux for 17 h, producing a yellow solution. The solvent was removed *in vacuo* to give a yellow residue, which was dissolved in CH_2Cl_2 (10 cm^3) and CF_3SO_3H (0.1 mol dm^{-3}) in methanol (3 cm^3, 0.3 mmol) added, and heated to reflux for 16 h. The solvent was evaporated *in vacuo* and the residue recrystallised from CH_2Cl_2–Et_2O. Yield of $[Ru_2(\mu\text{-}Cl)_3(AsMe_3)_4(PPh_3)_2][CF_3SO_3]$ 0.28 g (74%) (Found: C, 39.8; H, 4.5; Cl, 7.2. Calc. for $C_{49}H_{66}As_4Cl_3F_3O_3P_2Ru_2S$: C, 40.25; H, 4.55; Cl, 7.3%). ^1H NMR (CD_2Cl_2): δ 0.66 (3 H, s, CH_3), 1.16 (3 H, s, CH_3) and 7.35 (5 H, m, C_6H_5). ^{31}P-{^1H} NMR (CD_2Cl_2): δ +53.2.

(8) Tri-μ-chloro-bis[tris(trimethylphosphine)ruthenium(II)] triflate. Prepared as in (1) by heating $K_3[Ru_2Cl_9]$ (0.20 g, 0.31 mmol) and PMe_3 (0.25 g, 3.3 mmol) in ethanol (40 cm^3) and water (10 cm^3) for 40 h. Yield of $[Ru_2(\mu\text{-}Cl)_3(PMe_3)_6][CF_3SO_3]$ 0.14 g (49%) (Found: C, 25.3; H, 6.1; Cl, 11.8. $C_{19}H_{54}Cl_3F_3O_3P_6Ru_2S$ requires C, 25.0; H, 5.95; Cl, 11.6%). ^{31}P-{^1H} NMR (CD_2Cl_2): δ +22.2.

(9) Tri-μ-bromo-bis[tris(trimethylphosphine)ruthenium(II)] triflate. Prepared as in (1) by heating $K_3[Ru_2Br_9]$ (0.15 g, 0.14 mmol) and PMe_3 (0.15 g, 2.0 mmol) in ethanol (40 cm^3) and water (10 cm^3) for 16 h. Yield of $[Ru_2(\mu\text{-}Br)_3(PMe_3)_6][CF_3SO_3]$ 0.056 g (38%) (Found: C, 21.9; H, 5.3; Br, 22.8. $C_{19}H_{54}Br_3F_3O_3P_6Ru_2S$ requires C, 21.8; H, 5.2; Br, 22.9%). ^{31}P-{^1H} NMR (CD_2Cl_2): δ +19.6.

(10) Tri-μ-chloro-bis[tris(dimethylphenylphosphine)ruthenium(II)] triflate. To a suspension of $[RuCl_2(PPh_3)_3]$ (0.25 g, 0.26 mmol) in ethanol (30 cm^3) was added PMe_2Ph (0.15 g, 1.09 mmol). The mixture was heated at reflux for 90 h, producing a yellow solution. The solvent was removed *in vacuo* to give a yellow residue, which was stirred with a mixture of benzene (2 cm^3) and Et_2O (10 cm^3) to give a yellow precipitate {$[Ru_2(\mu\text{-}Cl)_3(PMe_2Ph)_6]Cl$} which was collected and washed with Et_2O. The chloride salt was dissolved in CH_2Cl_2 (10 cm^3) and CF_3SO_3H (0.1 mol dm^{-3}) in methanol (2 cm^3, 0.2 mmol) added, and heated to reflux for 16 h. The solvent was evaporated *in vacuo* and the residue recrystallised from CH_2Cl_2–Et_2O to give yellow crystalline $[Ru_2(\mu\text{-}Cl)_3(PMe_2Ph)_6][CF_3SO_3]$. Yield: 0.30 g (90%) (Found: C, 45.8; H, 5.0; Cl, 8.5. $C_{49}H_{66}Cl_3F_3O_3P_6Ru_2S$ requires C, 45.75; H, 5.2; Cl, 8.3%). ^{31}P-{^1H} NMR (CD_2Cl_2): δ +21.0.

(11) Tri-μ-bromo-bis[tris(dimethylphenylphosphine)ruthenium(II)] triflate. Prepared as in (10), heating $[RuBr_2(PPh_3)_3]$ (0.25 g, 0.24 mmol) and PMe_2Ph (0.15 g, 1.09 mmol) in ethanol (30 cm^3) for 4 h. Yield of $[Ru_2(\mu\text{-}Br)_3(PMe_2Ph)_6][CF_3SO_3]$ 0.31 g (91%) (Found: C, 40.9; H, 4.7; Br, 17.3. $C_{49}H_{66}Br_3F_3O_3P_6Ru_2S$ requires C, 41.45; H, 4.7; Br, 16.9%). ^{31}P-$\{^1H\}$ NMR (CD_2Cl_2): δ +18.9.

(12) Tri-μ-chloro-bis[tris(methyldiphenylphosphine)ruthenium(II)] triflate. Prepared as in (1) by heating $K_3[Ru_2Cl_9]$ (0.20 g, 0.31 mmol) and $PMePh_2$ (0.70 g, 3.5 mmol) in ethanol (40 cm^3) for 72 h. Yield of $[Ru_2(\mu\text{-}Cl)_3(PMe_3)_6][CF_3SO_3]$ 0.30 g (58%) (Found: C, 56.6; H, 4.7; Cl, 6.3. $C_{79}H_{78}Cl_3F_3O_3P_6Ru_2S$ requires C, 57.2; H, 4.7; Cl, 6.4%). ^{31}P-$\{^1H\}$ NMR (CD_2Cl_2): δ +18.8.

(13) Tri-μ-chloro-bis[tris(triethylphosphine)ruthenium(II)] triflate. Prepared as in (10) by heating $[RuCl_2(PPh_3)_3]$ (0.25 g, 0.26 mmol) and PEt_3 (0.12 g, 1.02 mmol) in ethanol (30 cm^3) for 72 h. Yield of $[Ru_2(\mu\text{-}Cl)_3(PEt_3)_6][CF_3SO_3]$ 0.27 g (89%) (Found: C, 38.2; H, 8.2; Cl, 9.2. $C_{37}H_{90}Cl_3F_3O_3P_6Ru_2S$ requires C, 38.1; H, 7.8; Cl, 9.1%). ^{31}P-$\{^1H\}$ NMR (CD_2Cl_2): δ +33.7.

(14) Tri-μ-bromo-bis[tris(triethylphosphine)ruthenium(II)] triflate. Prepared as in (10) by heating $[RuBr_2(PPh_3)_3]$ (0.25 g, 0.24 mmol) and PEt_3 (0.12 g, 1.02 mmol) in ethanol (30 cm^3) for 8 h. Yield of $[Ru_2(\mu\text{-}Br)_3(PEt_3)_6][CF_3SO_3]$ 0.22 g (71%) (Found: C, 34.0; H, 7.2; Br, 18.7. $C_{37}H_{90}Br_3F_3O_3P_6Ru_2S$ requires C, 34.2; H, 7.0; Br, 18.4%). ^{31}P-$\{^1H\}$ NMR (CD_2Cl_2): δ +33.5.

(15) Tri-μ-chloro-bis[tris(diethylphenylphosphine)ruthenium(II)] triflate. Prepared as in (10) by heating $[RuCl_2(PPh_3)_3]$ (0.25 g, 0.26 mmol) and PEt_2Ph (0.17 g, 1.02 mmol) in ethanol (30 cm^3) for 85 h. Yield of $[Ru_2(\mu\text{-}Cl)_3(PEt_2Ph)_6][CF_3SO_3]$ 0.31 g (82%) (Found: C, 49.1; H, 6.3; Cl, 6.8. $C_{61}H_{90}Cl_3F_3O_3P_6Ru_2S$ requires C, 50.4; H, 6.2; Cl, 7.3%). ^{31}P-$\{^1H\}$ NMR (CD_2Cl_2): δ +36.0.

(16) Tri-μ-bromo-bis[tris(diethylphenylphosphine)ruthenium(II)] triflate. Prepared as in (1) by heating $K_3[Ru_2Br_9]$ (0.20 g, 0.19 mmol) and PEt_2Ph (0.40 g, 2.4 mmol) in ethanol (40 cm^3) for 16 h. Yield of $[Ru_2(\mu\text{-}Br)_3(PEt_2Ph)_6][CF_3SO_3]$ 0.18 g (58%) (Found: C, 46.3; H, 6.3; Br, 15.1. $C_{61}H_{90}Br_3F_3O_3P_6Ru_2S$ requires C, 46.1; H, 5.7; Br, 15.1%). ^{31}P-$\{^1H\}$ NMR (CD_2Cl_2): δ +35.1.

(17) Tri-μ-chloro-bis[tris(ethyldiphenylphosphine)ruthenium(II)] triflate. Prepared as in (10) by heating $[RuCl_2(PPh_3)_3]$ (0.25 g, 0.26 mmol) and $PEtPh_2$ (0.22 g, 1.03 mmol) in ethanol (30 cm^3) for 56 h. Yield of $[Ru_2(\mu\text{-}Cl)_3(PEtPh_2)_6][CF_3SO_3]$ 0.13 g (29%) (Found: C, 58.0; H, 5.6; Cl, 7.2. $C_{85}H_{90}Cl_3F_3O_3P_6Ru_2S$ requires C, 58.6; H, 5.2; Cl, 6.1%). ^{31}P-$\{^1H\}$ NMR (CD_2Cl_2): δ +33.3.

(18) Tri-μ-chloro-bis{[1,1,1-tris(diphenylphosphinomethyl)-ethane]ruthenium(II)} triflate. Prepared as in (10) by heating $[RuCl_2(PPh_3)_3]$ (0.25 g, 0.26 mmol) and $MeC(CH_2PPh_2)_3$ (0.32 g, 0.54 mmol) in 2-methoxyethanol (30 cm^3) for 6 h. Yield of $[Ru_2(\mu\text{-}Cl)_3\{MeC(CH_2PPh_2)_3\}_2][CF_3SO_3]$ 0.44 g (99%) (Found: C, 58.8; H, 4.9; Cl, 6.4. $C_{83}H_{78}Cl_3F_3O_3P_6Ru_2S$ requires C, 58.4; H, 4.6; Cl, 6.2%). ^{31}P-$\{^1H\}$ NMR (CD_2Cl_2): δ +36.5.

(19) Tri-μ-bromo-bis{[1,1,1-tris(diphenylphosphinomethyl)-ethane]ruthenium(II)} triflate. Prepared as in (10) by heating $[RuBr_2(PPh_3)_3]$ (0.25 g, 0.24 mmol) and $MeC(CH_2PPh_2)_3$ (0.30 g, 0.50 mmol) in 2-methoxyethanol (30 cm^3) for 26 h. Yield of $[Ru_2(\mu\text{-}Br)_3\{MeC(CH_2PPh_2)_3\}_2][CF_3SO_3]$ 0.26 g (59%) (Found: C, 53.9; H, 4.0; Br, 13.2. $C_{83}H_{78}Br_3F_3O_3P_6Ru_2S$ requires C, 54.2; H, 4.3; Br, 13.0%). ^{31}P-$\{^1H\}$ NMR (CD_2Cl_2): δ +32.6.

(20) Tri-μ-chloro-bis[tris(methyl diphenylphosphinite)ruthenium(II)] triflate. Prepared as in (10) by heating $[RuCl_2(PPh_3)_3]$ (0.25 g, 0.26 mmol) and $P(OMe)Ph_2$ (0.22 g, 1.02 mmol) in methanol (30 cm^3) for 4 h. Yield of $[Ru_2(\mu\text{-}Cl)_3\{P(OMe)Ph_2\}_6][CF_3SO_3]$ 0.41 g (90%) (Found: C, 53.6; H, 4.4; Cl, 6.9. Calc. for $C_{79}H_{78}Cl_3F_3O_9P_6Ru_2S$: C, 54.1; H, 4.5; Cl, 6.1%). ^{31}P-$\{^1H\}$ NMR (CD_2Cl_2): δ +138.7.

Acknowledgements

We thank the Institute of Advanced Studies (ANU) for support, the Commonwealth Government for Australian Postgraduate Awards (to D. G. H. and B. D. Y.), Professor K. Wieghardt for the gift of tmtacn complexes, Mr. S. B. Lee for technical assistance and Mr. C. Tomkins for building the jacketed electrolysis cell. We thank the following colleagues for many helpful discussions, and for permission to draw on data in advance of publication: Drs. L. Dubicki and J. E. McGrady for theoretical analyses, Dr. D. C. R. Hockless for X-ray structural measurements, and Drs. S. Boyd, R. Bramley and P. D. Prenzler for the extensive EPR measurements to be detailed elsewhere.

References

1 B. D. Yeomans, Ph.D. Thesis, *Mixed-valency in Confacial Bioctahedral Complexes of Ruthenium and Osmium*, The Australian National University, 1995.
2 D. G. Humphrey, Ph.D. Thesis, *Binuclear Osmium Complexes and Related Complexes*, The Australian National University, 1992.
3 E. A. Seddon and K. R. Seddon, *The Chemistry of Ruthenium*, Elsevier, Amsterdam, 1984; M. Schröder and T. A. Stephenson, in *Comprehensive Coordination Chemistry*, ed. G. Wilkinson, Pergamon, New York, 1987, vol. 4, ch. 45, pp. 277–518; F. A. Cotton and R. A. Walton, *Multiple Bonds between Metal Atoms*, Oxford University Press, 2nd edn., 1993, pp. 600–606.
4 G. A. Heath and J. E. McGrady, *J. Chem. Soc.*, *Dalton Trans.*, 1994, 3759.
5 E. E. Mercer and P. E. Dumas, *Inorg. Chem.*, 1971, **10**, 2755; E. E. Mercer and L. W. Gray, *J. Am. Chem. Soc.*, 1972, **94**, 6426.
6 J. Chatt and R. G. Hayter, *J. Chem. Soc.*, 1961, 896.
7 G. A. Heath, A. J. Lindsay, T. A. Stephenson and D. K. Vattis, *J. Organomet. Chem.*, 1982, **233**, 353.
8 B. J. Kennedy, G. A. Heath and T. J. Khoo, *Inorg. Chim. Acta*, 1991, **190**, 672.
9 R. H. Summerville and R. Hoffmann, *J. Am. Chem. Soc.*, 1979, **101**, 3821; W. C. Trogler, *Inorg. Chem.*, 1980, **19**, 697.
10 N. S. Hush, J. K. Beattie and V. M. Ellis, *Inorg. Chem.*, 1984, **23**, 3339.
11 L. Dubicki and E. R. Kraus, *Inorg. Chem.*, 1985, **24**, 4461.
12 R. S. Armstrong, W. A. Horsfield and K. W. Nugent, *Inorg. Chem.*, 1990, **29**, 4551.
13 K. Wieghardt, W. Herrmann, M. Köppen, I. Jibril and G. Huttner, *Z. Naturforsch.*, *Teil B*, 1984, **39**, 1335.
14 P. Neubold, B. S. P. Della Vedova, K. Wieghardt, B. Nuber and J. Weiss, *Inorg. Chem.*, 1990, **29**, 3355.
15 W. A. Clucas, Ph.D. Thesis, University of Sydney, 1994; W. A. Clucas, R. S. Armstrong, I. E. Buys, T. W. Hambley and K. W. Nugent, *Inorg. Chem.*, 1996, **35**, 6789.
16 G. A. Heath, G. Hefter, D. R. Robertson, W. J. Sime and T. A. Stephenson, *J. Organomet. Chem.*, 1978, **152**, C1.
17 T. Arthur, R. Contreras, G. A. Heath, G. Hefter, A. J. Lindsay, D. J. Riach and T. A. Stephenson, *J. Organomet. Chem.*, 1979, **179**, C49.
18 S. A. Macgregor, E. McInnes, R. J. Sorbie and L. J. Yellowlees, in *Molecular Electrochemistry of Inorganic*, *Bioinorganic and Organometallic Compounds*, Eds. A. J. L. Pombeiro and J. A. McCleverty, NATO ASI Series C, Kluwer, Dordrecht, 1993, vol. 345, pp. 503–517.
19 M. S. Lupin and B. L. Shaw, *J. Chem. Soc. A*, 1968, 741.
20 D. A. Couch and S. D. Robinson, *Inorg. Chem.*, 1974, **13**, 456.
21 P. W. Armit, A. S. F. Boyd and T. A. Stephenson, *J. Chem. Soc.*, *Dalton Trans.*, 1975, 1663.
22 M. Laing and L. Pope, *Acta Crystallogr.*, *Sect. B*, 1976, **32**, 1547.
23 W. J. Sime and T. A. Stephenson, *J. Organomet. Chem.*, 1977, **124**, C23.
24 K. A. Raspin, *J. Chem. Soc. A*, 1969, 461.
25 L. F. Rhodes, C. Sorato, L. M. Venanzi and F. Bachechi, *Inorg. Chem.*, 1988, **27**, 604.
26 G. Albertin, S. Antoniutti and E. Bordignon, *J. Chem. Soc.*, *Dalton Trans.*, 1987, 1813.

27 A. Albinati, Q. Jiang, H. Rügger and L. M. Venanzi, *Inorg. Chem.*, 1993, **32**, 4940.
28 E. G. Leelamani and G. K. N. Reddy, *Inorg. Nucl. Chem. Lett.*, 1975, **11**, 5.
29 K. G. Srinivasamurthy, N. M. Nanje-Gowda and G. K. N. Reddy, *J. Inorg. Nucl. Chem.*, 1977, **39**, 1977.
30 V. T. Coombe, G. A. Heath, T. A. Stephenson and D. K. Vattis, *J. Chem. Soc.*, *Dalton Trans.*, 1983, 2307.
31 J. E. Fergusson and A. M. Greenaway, *Aust. J. Chem.*, 1978, **31**, 497.
32 J. Chatt, B. L. Shaw and A. E. Field, *J. Chem. Soc.*, 1964, 3466.
33 A. J. Lindsay, Ph.D. Thesis, *Redox-active Binuclear Complexes of Ruthenium and Osmium*, University of Edinburgh, 1982.
34 C. Shi and F. C. Anson, *Inorg. Chim. Acta*, 1994, **225**, 215.
35 L. D. Dubicki, unpublished work.
36 R. Contreras, G. G. Elliot, R. O. Gould, G. A. Heath and T. A. Stephenson, *J. Organomet. Chem.*, 1981, **215**, C6.
37 F. A. Cotton and R. C. Torralba, *Inorg. Chem.*, 1991, **30**, 2196.
38 N. S. Hush, A. Edgar and J. K. Beattie, *Chem. Phys. Lett.*, 1980, **69**, 128.
39 N. S. Hush, in *Mixed Valence Compounds*, ed. D. B. Brown, Reidel, Dordrecht, 1980, pp. 151–188.
40 S. E. Boyd, R. Bramley, L. Dubicki, G. A. Heath, D. G. Humphrey, P. D. Prenzler and B. D. Yeomans, unpublished work.
41 G. A. Heath, D. C. R. Hockless and B. D. Yeomans, *Acta Crystallogr.*, *Sect. C*, 1996, **52**, 854.
42 D. C. R. Hockless, B. D. Yeomans and G. A. Heath, unpublished work.
43 J. A. Statler, G. Wilkinson, M. Thornton-Pett and M. B. Hursthouse, *J. Chem. Soc.*, *Dalton Trans.*, 1984, 1731.
44 J. E. McGrady, Ph.D. Thesis, *Electronic Structure and Optical Spectra of Transition Metal Complexes*, The Australian National University, 1994.
45 M. N. Hughes, D. O'Reardon, R. K. Poole, M. B. Hursthouse and M. Thornton-Pett, *Polyhedron*, 1987, **6**, 1711.
46 J. K. Beattie, P. Del Favero, T. W. Hambley and N. S. Hush, *Inorg. Chem.*, 1988, **27**, 2000.
47 D. R. Gamelin, E. L. Bominaar, C. Mathoniére, M. L. Kirk, K. Wieghardt, J.-J. Girerd and E. I. Solomon, *Inorg. Chem.*, 1996, **35**, 4323.
48 J. E. Sutton, P. M. Sutton and H. Taube, *Inorg. Chem.*, 1979, **18**, 1017; C. Creutz, *Prog. Inorg. Chem.*, 1983, **30**, 1.
49 M. B. Robin and P. Day, *Adv. Inorg. Chem. Radiochem.*, 1967, **10**, 247.
50 G. A. Heath, J. E. McGrady, R. G. Raptis and A. C. Willis, *Inorg. Chem.*, 1996, **35**, 6838.
51 R. J. Crutchley, *Adv. Inorg. Chem.*, 1994, **41**, 273.
52 D. C. Ware, M. M. Olmstead, R. Wang and H. Taube, *Inorg. Chem.*, 1996, **35**, 2576.
53 G. A. Heath and D. G. Humphrey, *J. Chem. Soc.*, *Chem. Commun.*, 1990, 672.
54 S. F. Gheller, G. A. Heath, D. C. R. Hockless, D. G. Humphrey and J. E. McGrady, *Inorg. Chem.*, 1994, **33**, 3986.
55 N. J. Homes, A. R. G. Genge, W. Levason and M. Webster, *J. Chem. Soc.*, *Dalton Trans.*, 1997, 2331.
56 T. A. Stephenson and G. Wilkinson, *J. Inorg. Nucl. Chem.*, 1966, **28**, 945.
57 G. J. Burrows and E. E. Turner, *J. Chem. Soc.*, 1920, 1373.
58 M. L. Leutkens, A. P. Sattelberger, H. H. Murray, J. D. Basil and J. P. Fackler, *Inorg. Synth.*, 1989, **26**, 7.
59 C. M. Duff and G. A. Heath, *J. Chem. Soc.*, *Dalton Trans.*, 1991, 2401.

Received 10*th February* 1997; *Paper* 7/05675C